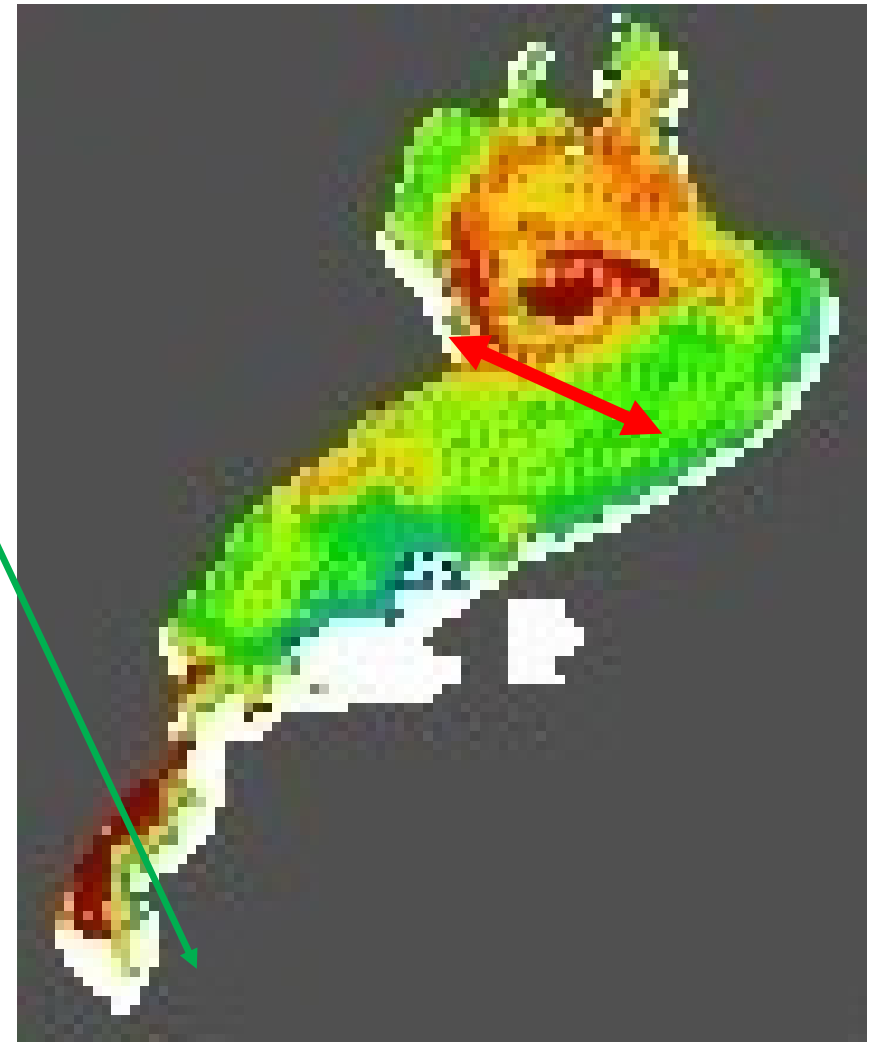


Part I (JpGU 18/5/22): Coastal Acoustic Tomography in Lake Biwa, Japan

*John WELLS, Tomonori OHARA, Hiroki UCHIDA
Ritsumeikan University

We will present results from a test of Coastal Acoustic Tomography (CAT) in Lake Biwa, Japan in November 2017. Three 5 kHz transducers were deployed along a 10.2 km line from the West Shore of the lake to Takeshima. Acoustic travel times between transducers are computed from correlograms of the emitted “M11” quasi-random code with the received signal. Small but consistent differences in travel times between reciprocal paths were observed, whence we estimate path-averaged currents along the dominant acoustic path on the order of 5 cm/s, which is not inconsistent with expected magnitudes at this site. For the temperature profile in November, ray paths pass almost entirely below the thermocline. To our knowledge this is the first reported estimate of currents by Acoustic Tomography in a lake.

Motivation: track/nowcast flow (thence pollutant *etc.*) in realtime

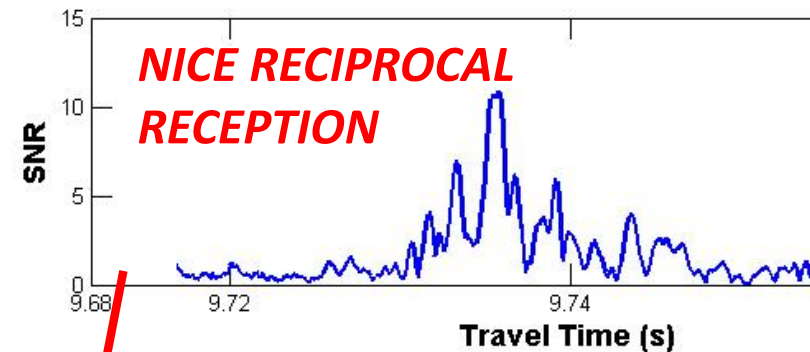
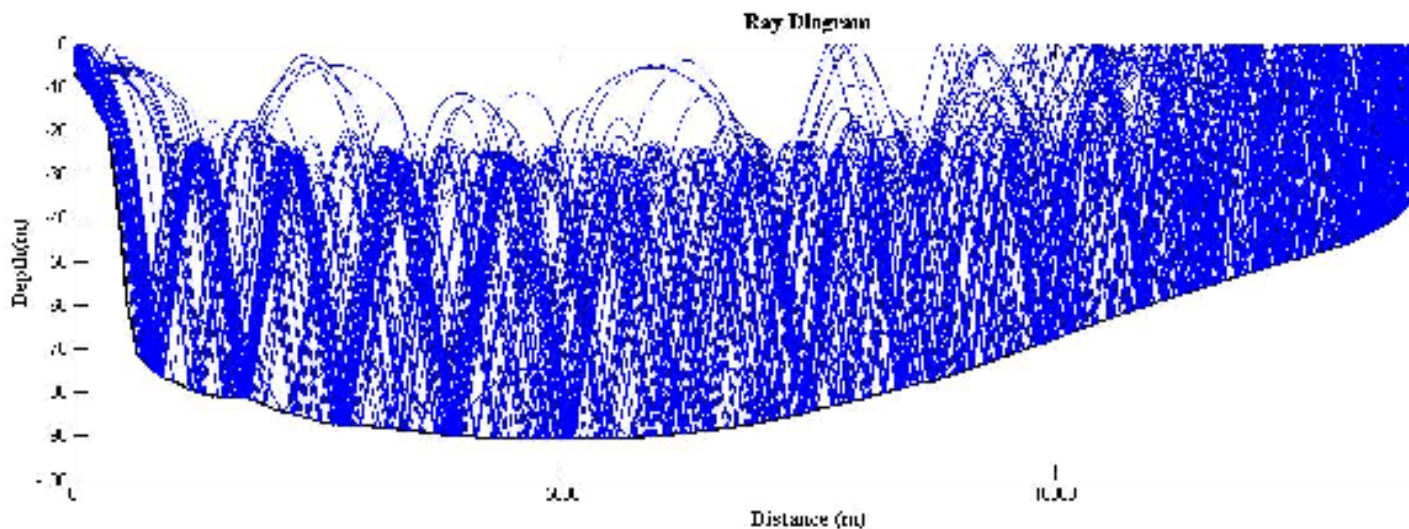


MODIS 2015/7/20/ 10:35 JST
“Chlorophyll a” (red: high conc.)

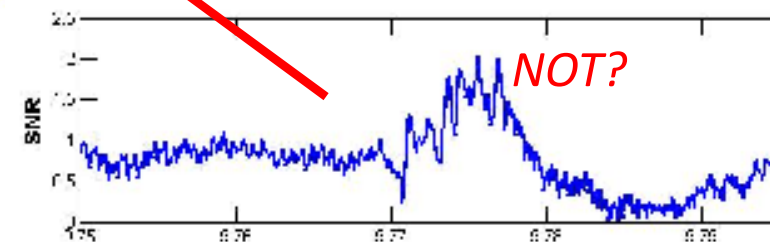
Application of Coastal Acoustic Tomography to Lake Biwa, Japan

John C. WELLS, Yasuaki AOTA, Guillaume AUGER
(Ritsumeikan U.), Arata KANEKO, Noriaki GODA (Hiroshima U.)

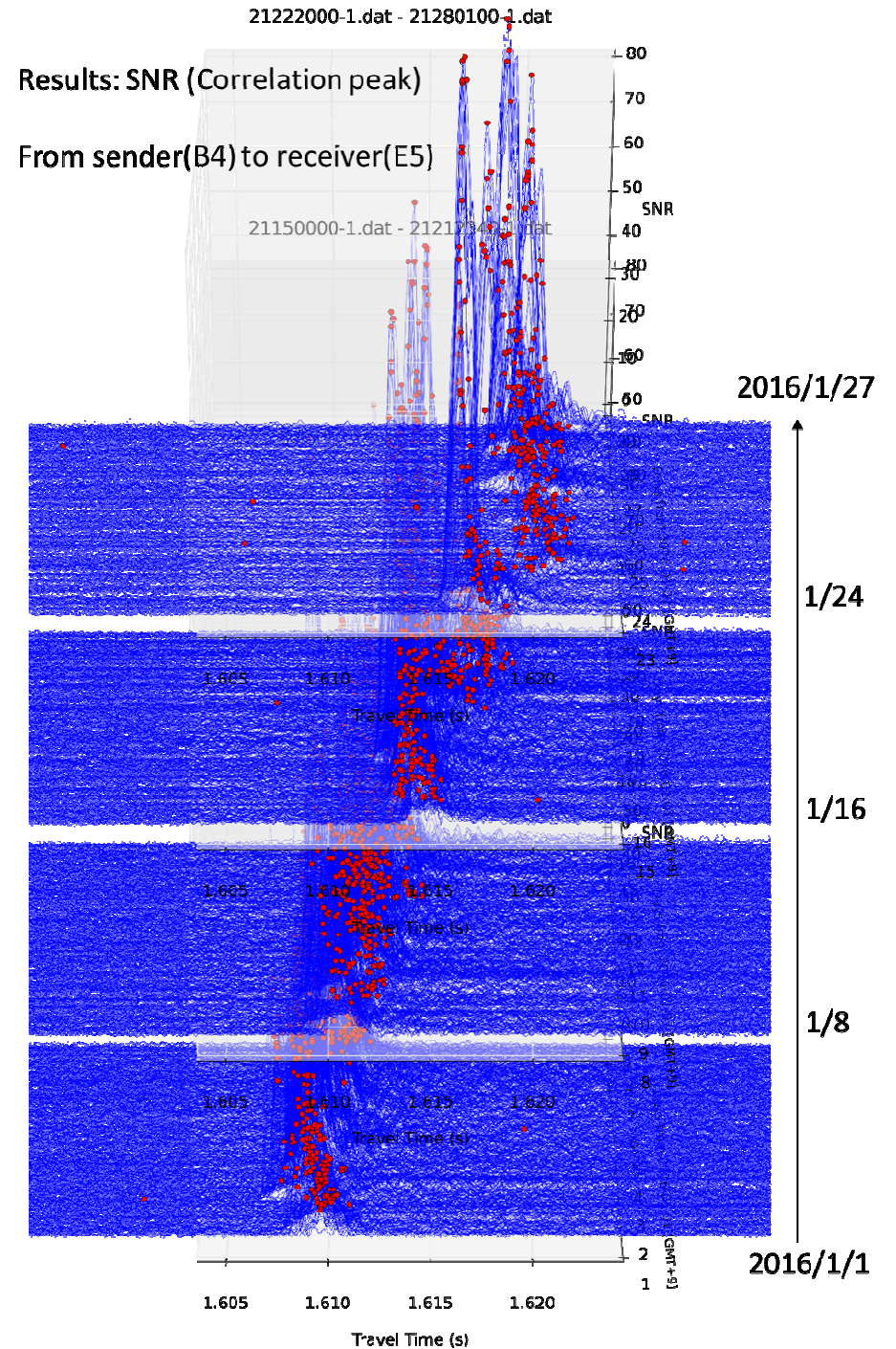
Coastal acoustic tomography (CAT) will provide monitoring data for assimilation into a prototype "nowcast system" for the flow and temperature fields in Lake Biwa, Japan. *→ aim for year-round installation capable of real-time data transfer and quasi-automated processing*



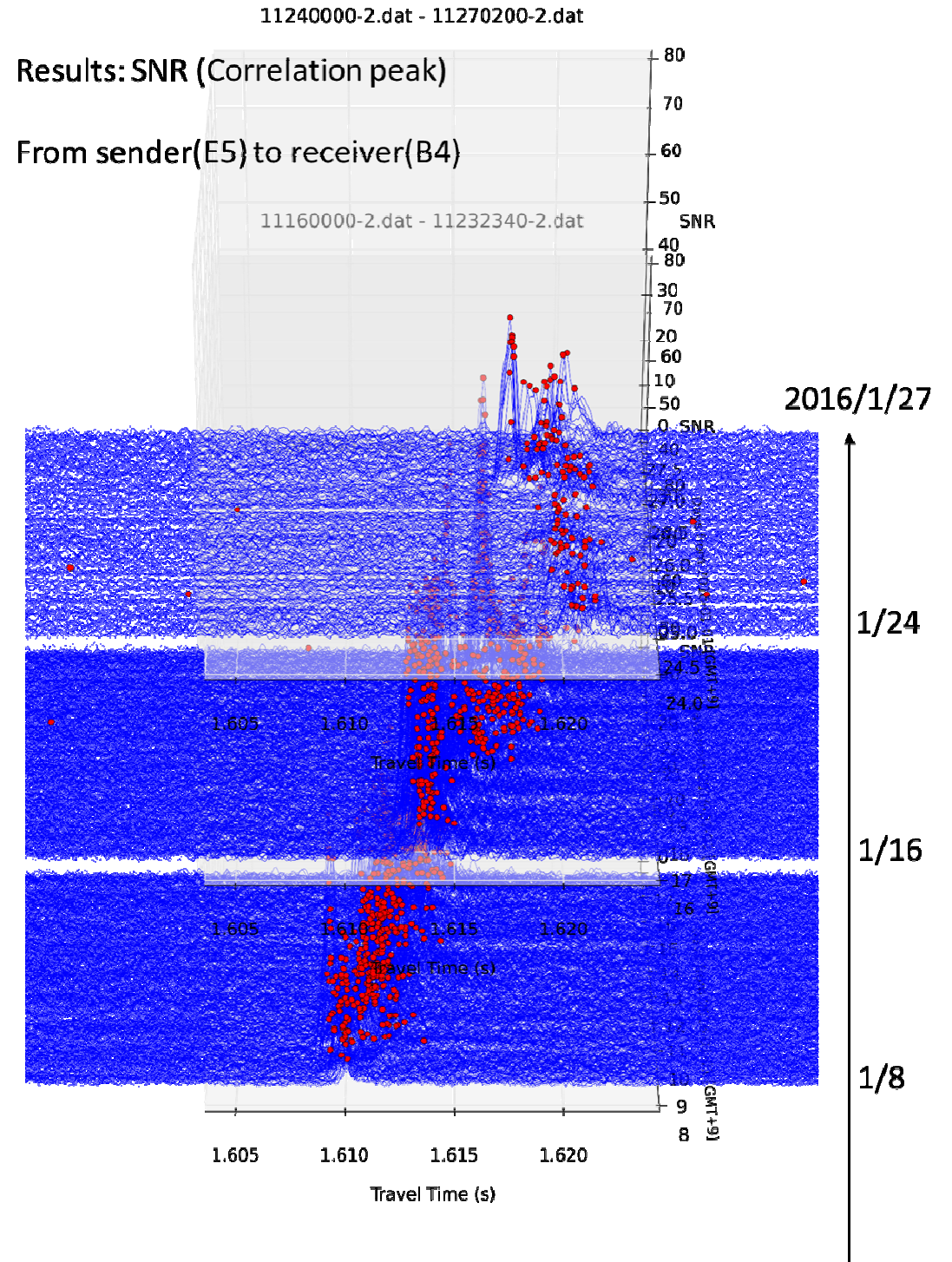
OR...



Part I.1. Continuous monitoring results in Jan. 2016. 5kHz carrier, M11, Q=3, no repeat, 20' intervals

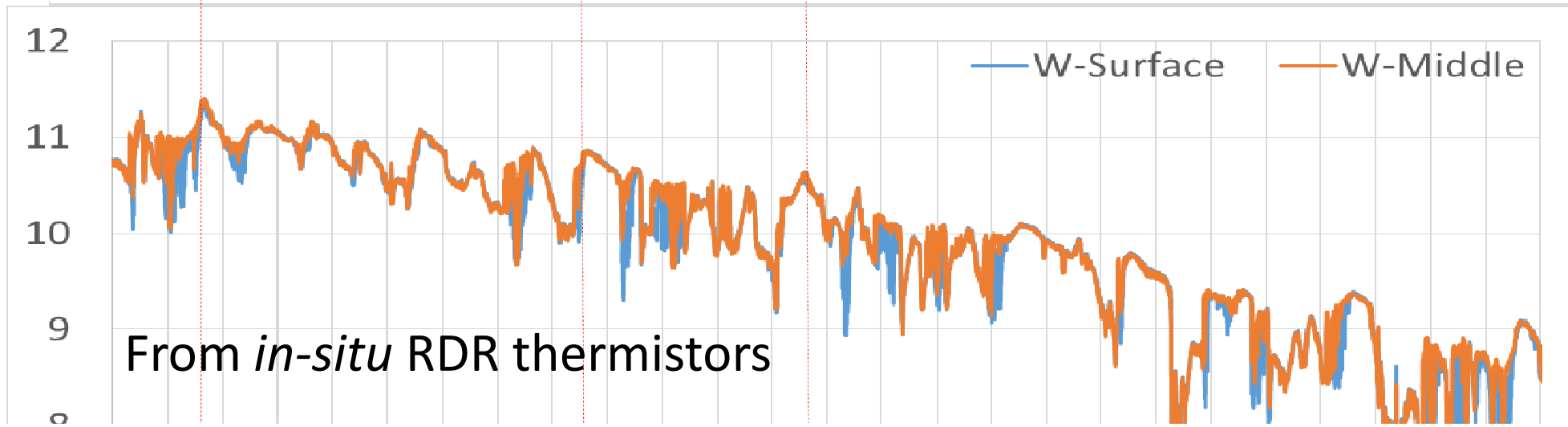
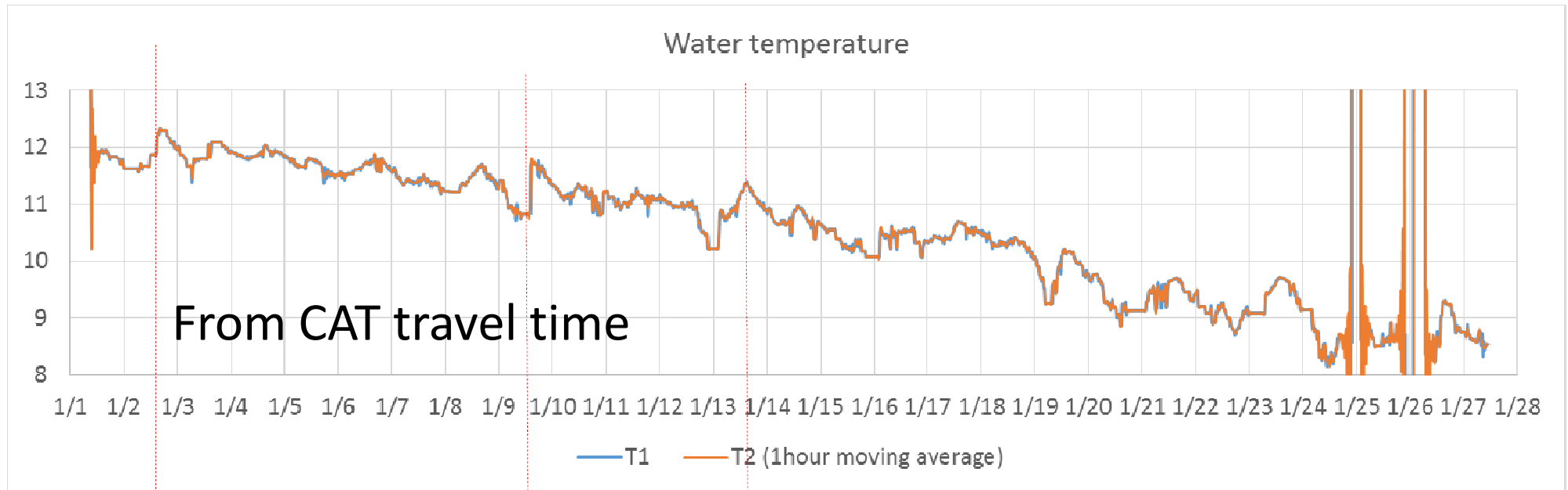


Part I. Continuous monitoring results in Jan. 2016. 5Hz carrier, M11, Q=3, no repeat, 20' intervals



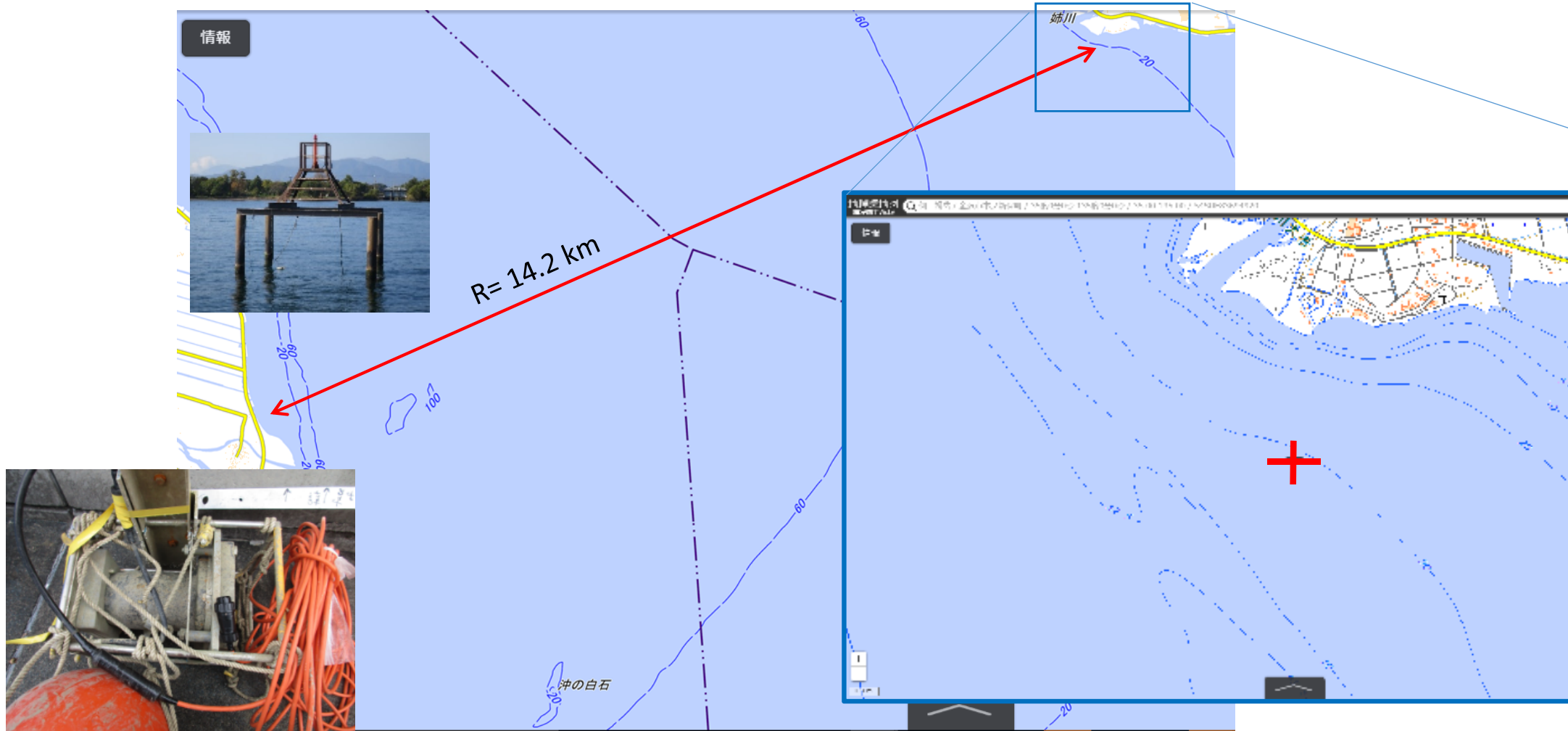
“Summary I.1” of CAT in L. Biwa

A two-month deployment between two TR (R=2.4 km, 20' intervals) has tracked the cooling in 4 to 9 m shallows in January 2016. Sudden temperature fluctuations were well captured.

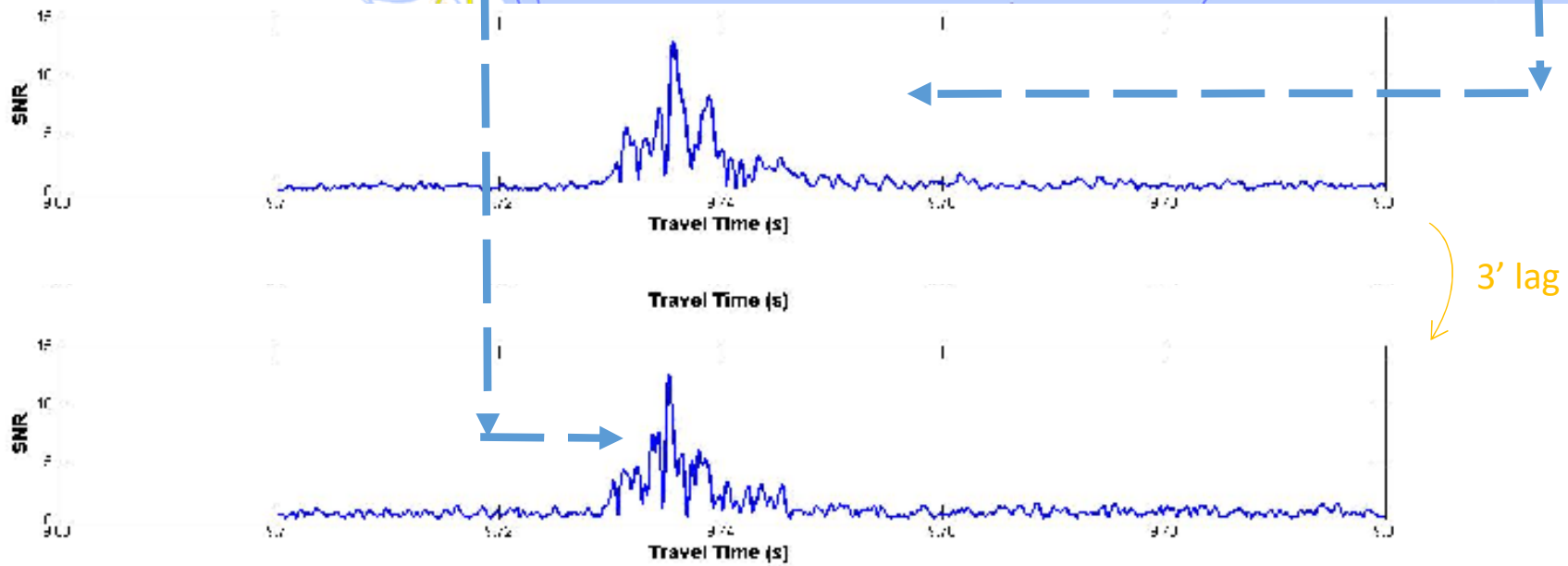
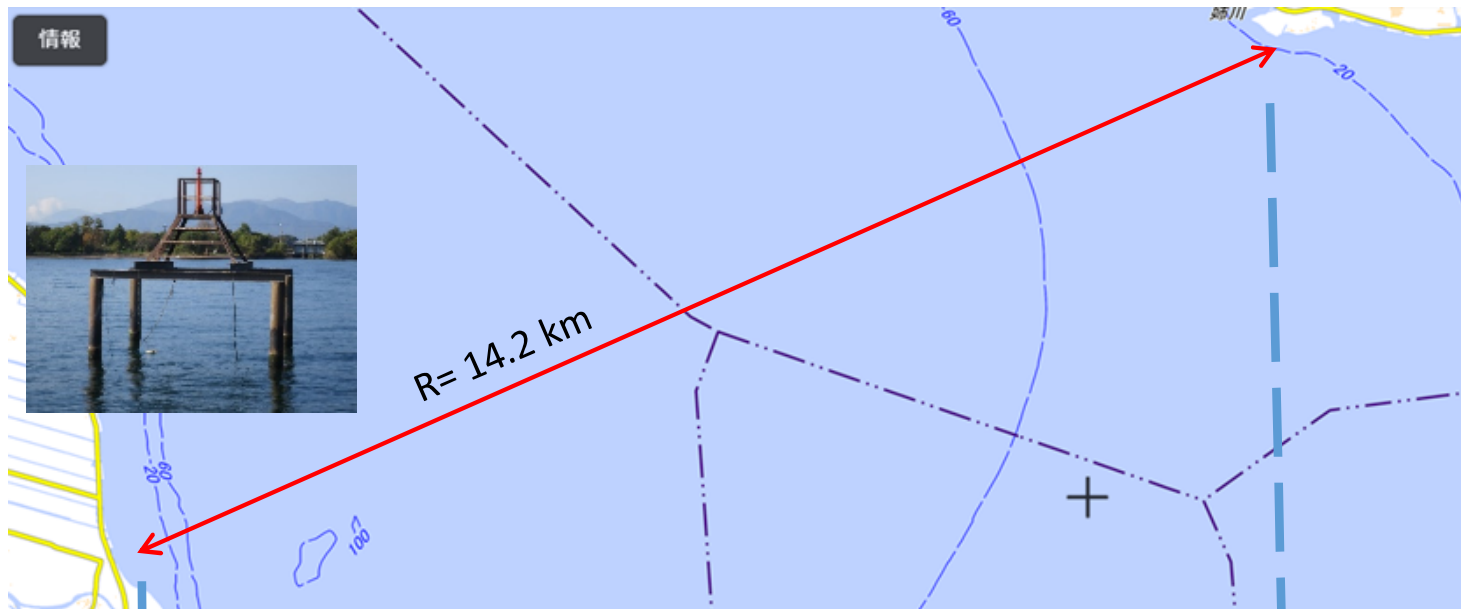


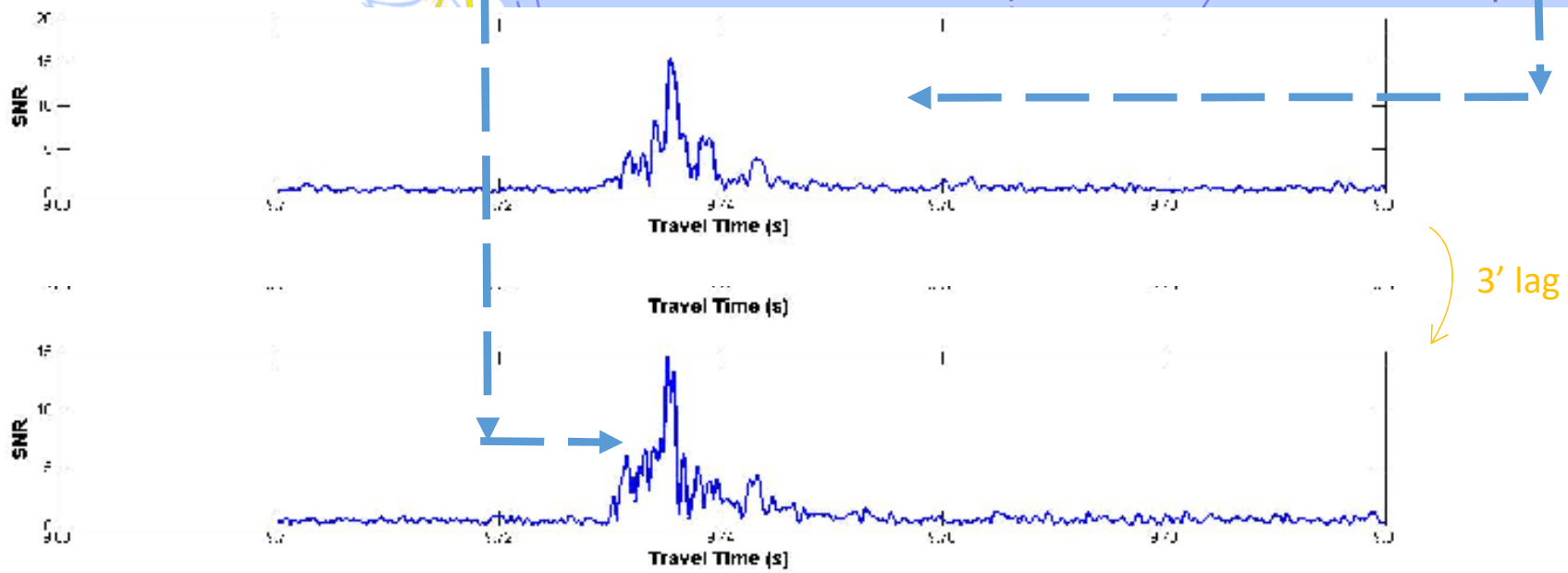
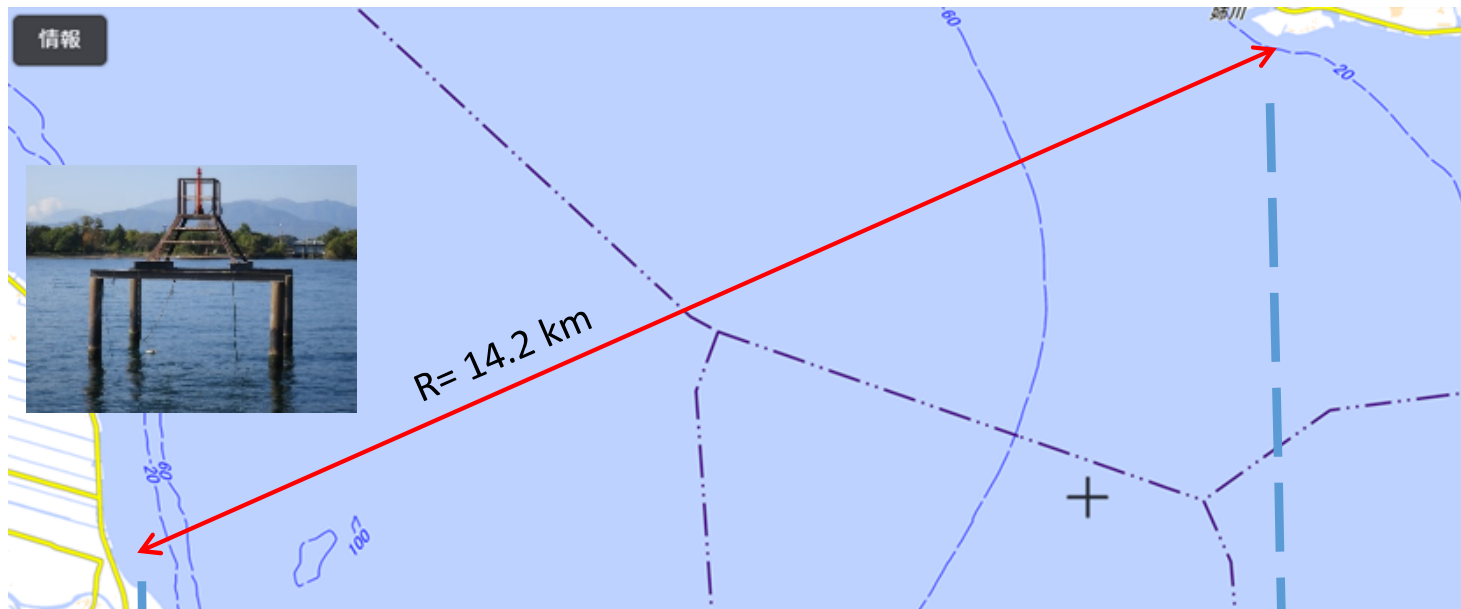
Part I.2. Basin-scale transmission under Stratified conditions Chronology

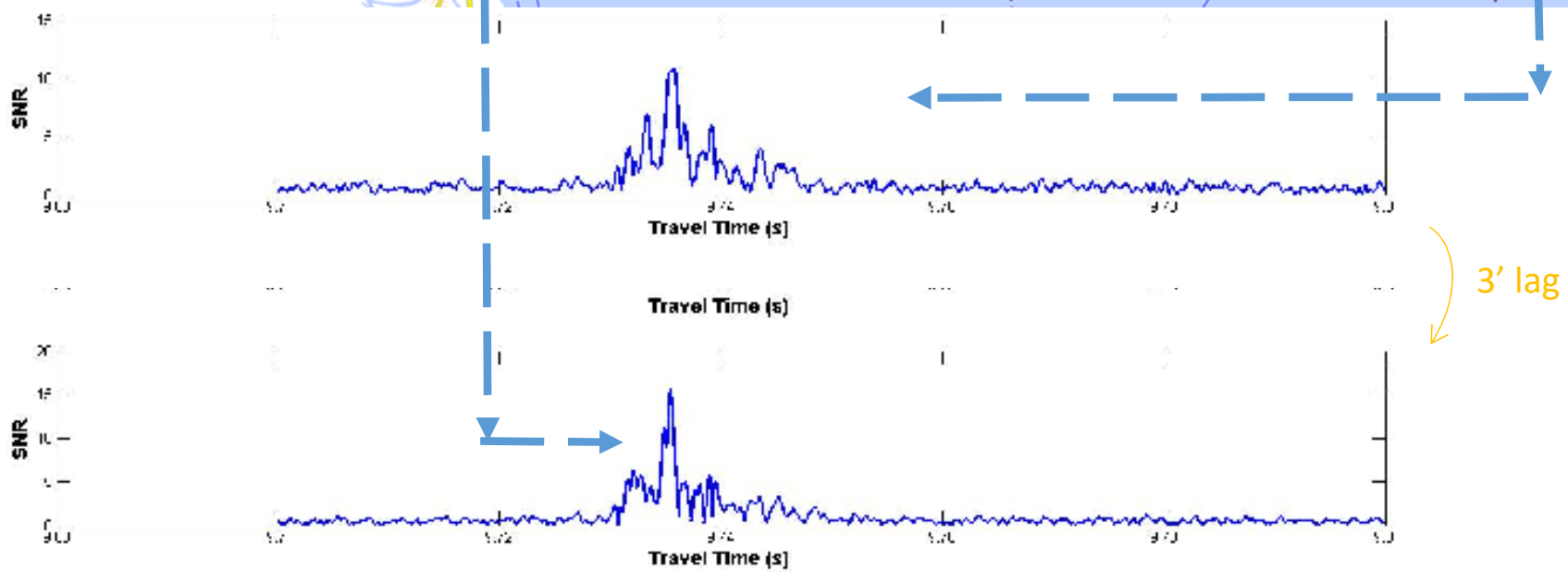
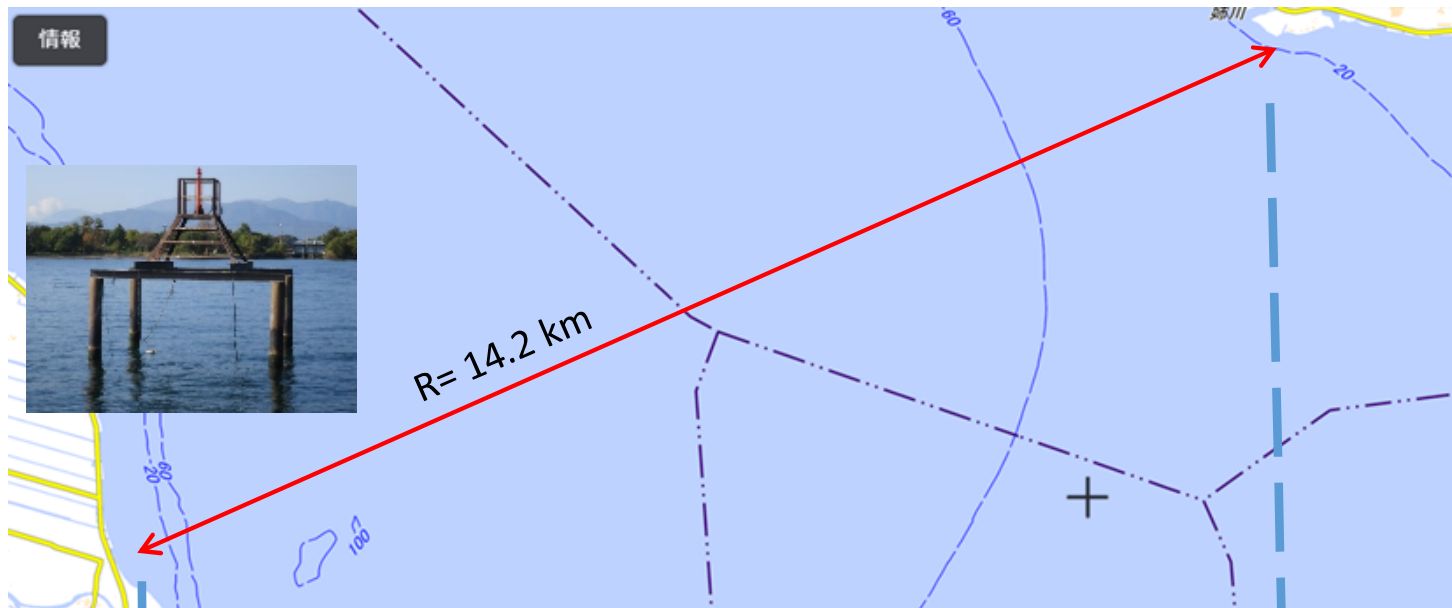
2) Using M11*6 repeat, reciprocal transmission was achieved between a TR fixed to the “Brown Tower” with a TR suspended 2.5 m above bottom (BD = 32 m), from an anchored vessel off the Ane River mouth on Nov 5.

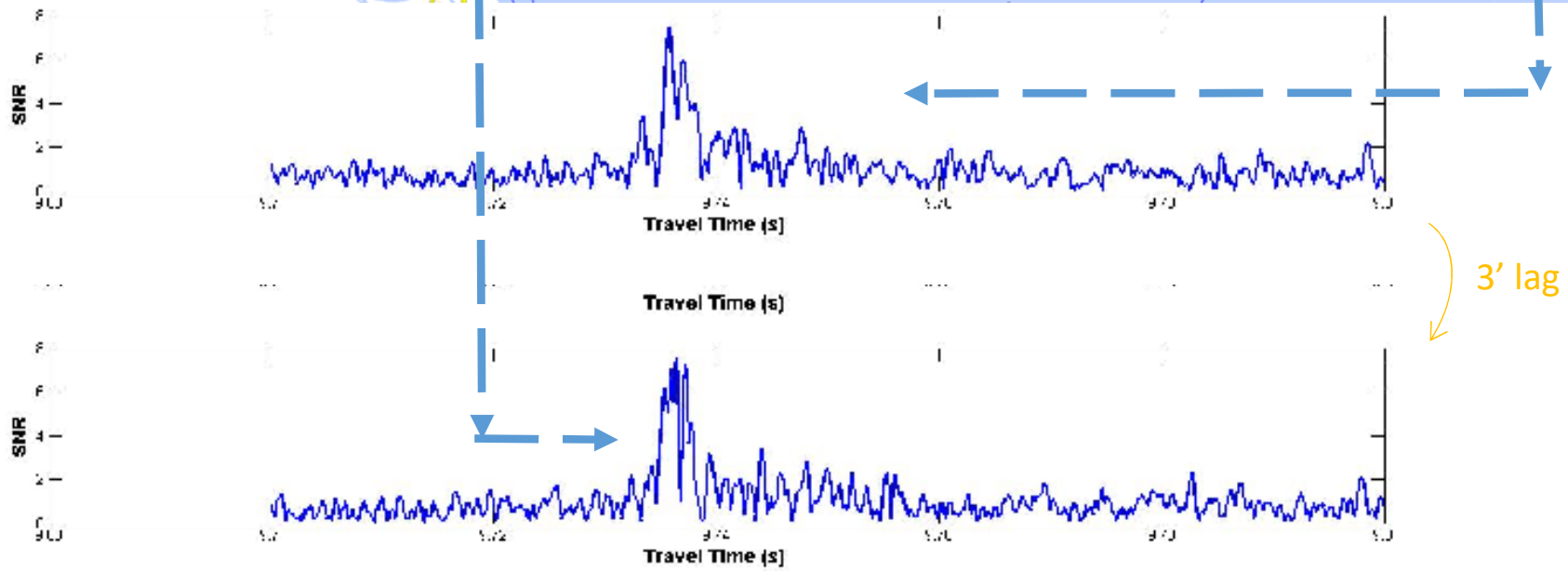
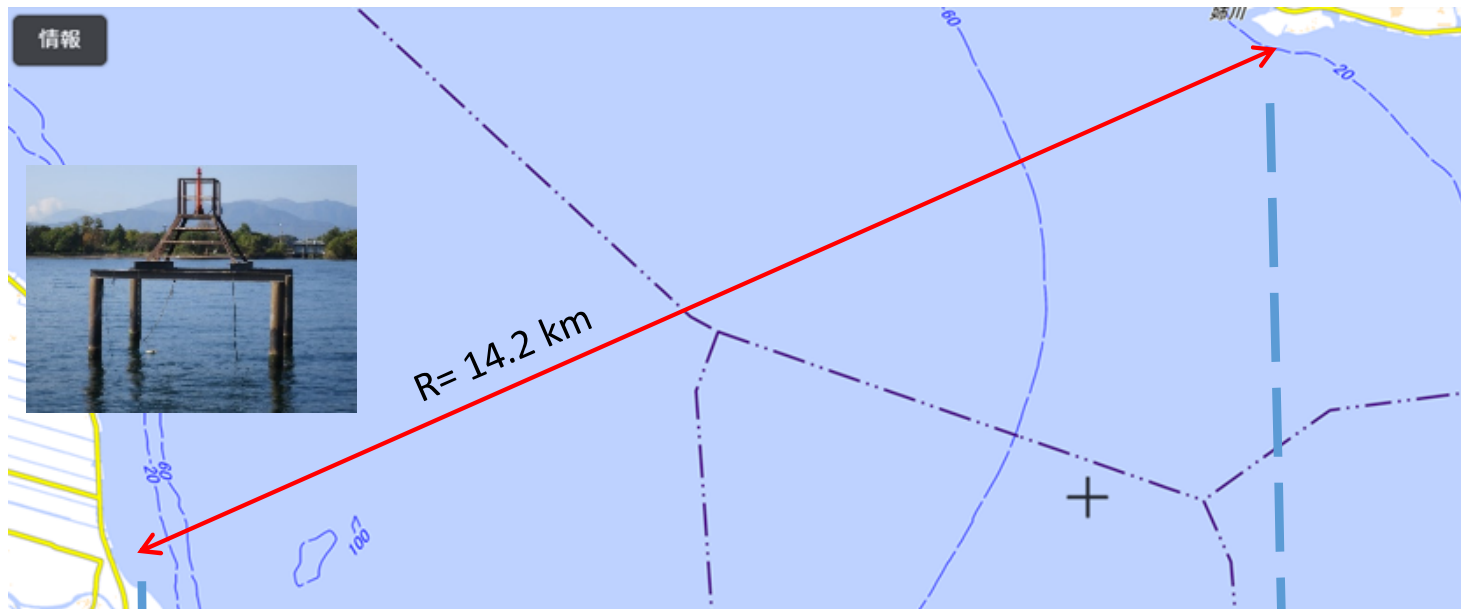


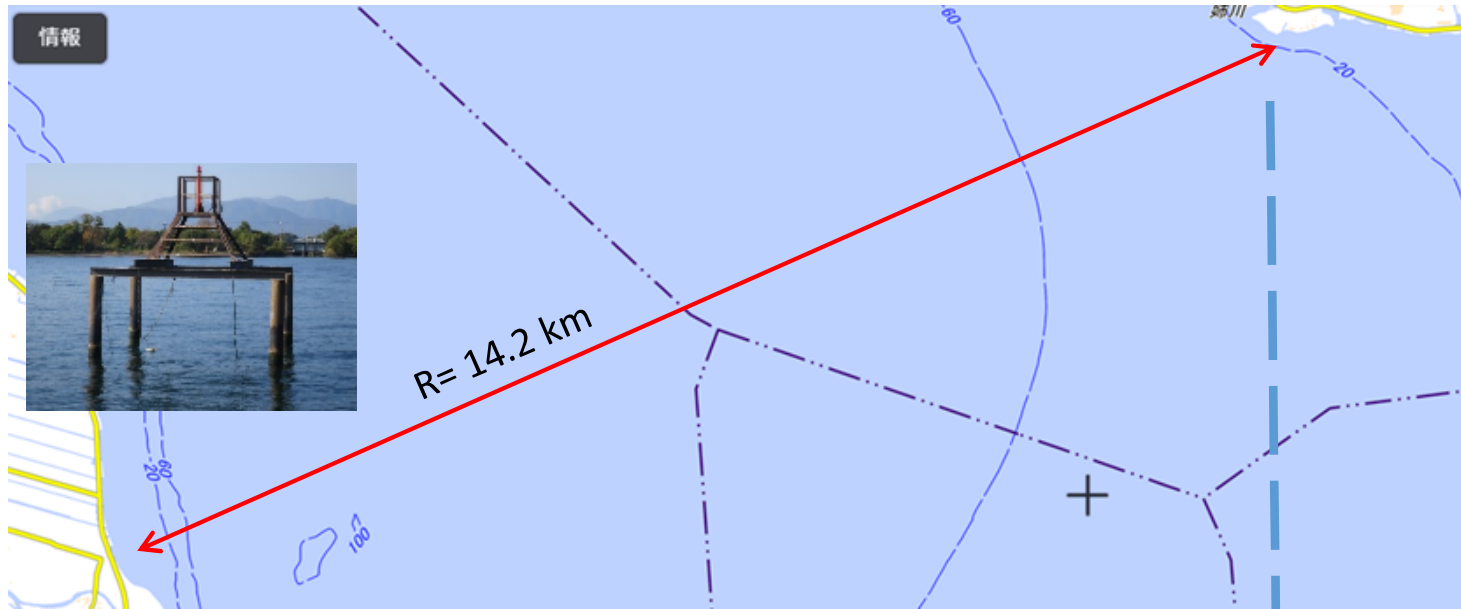
“directional” transducer











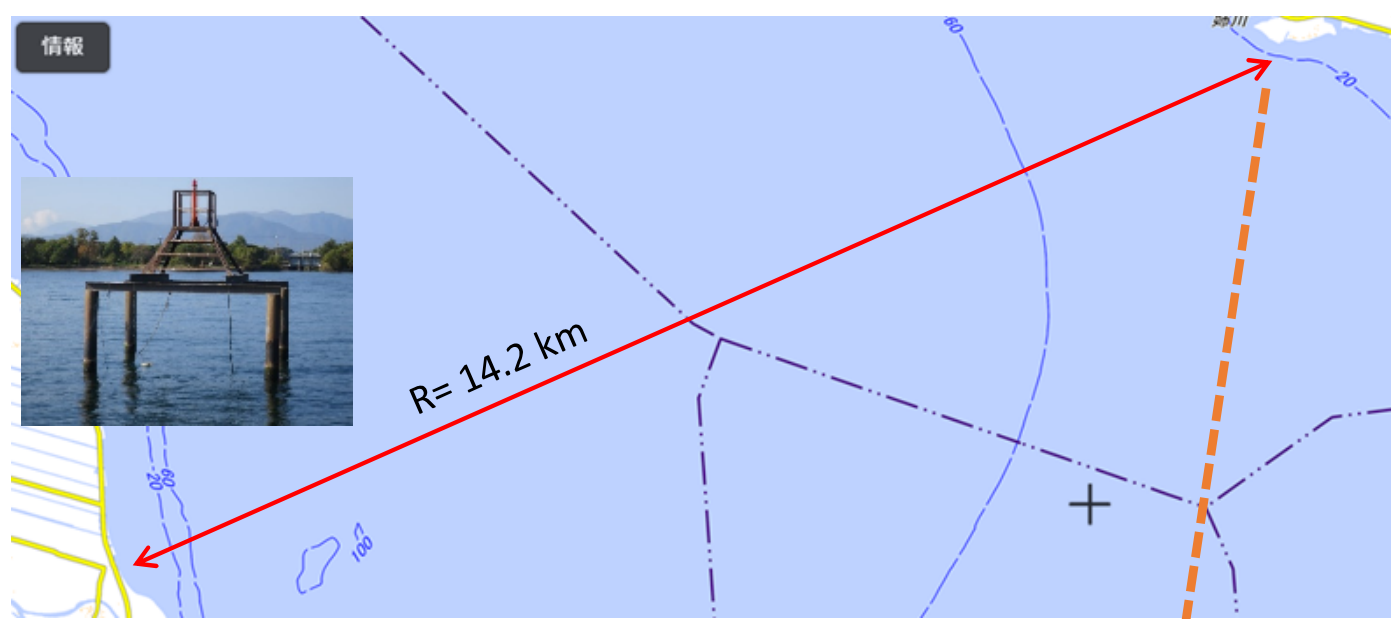
HOWEVER, on Nov 13, only the weakest of peaks was observed at the Ane River site with the TR suspended from an anchored vessel (BD =24 m, slightly shallower...)

Why ?

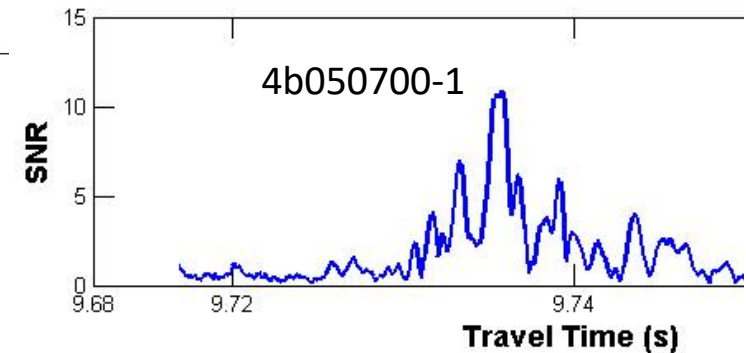
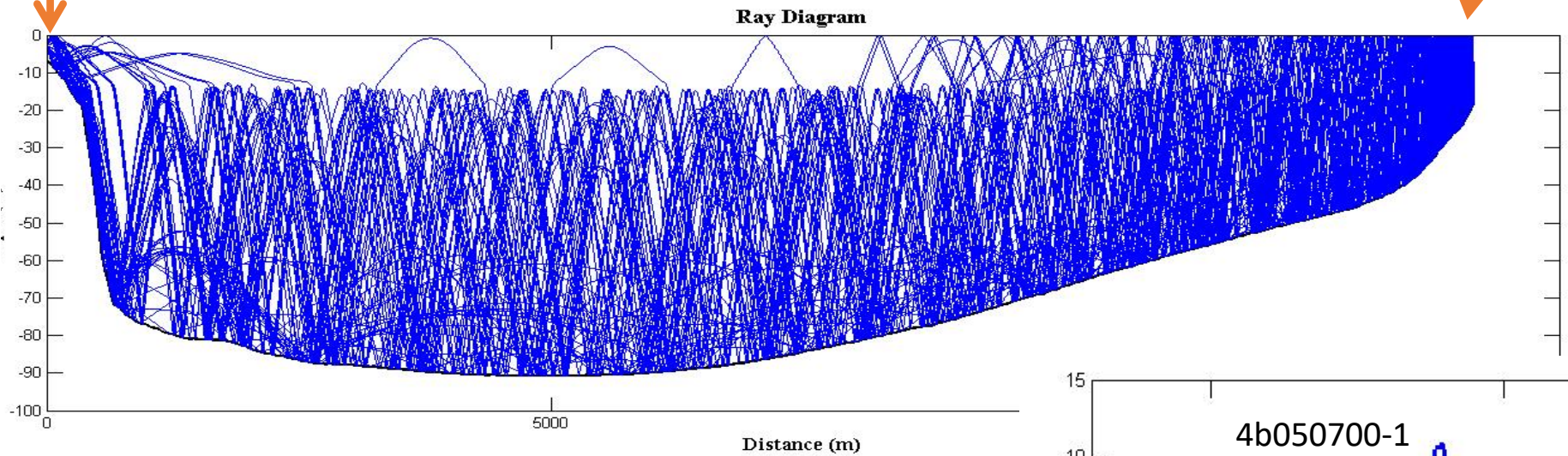
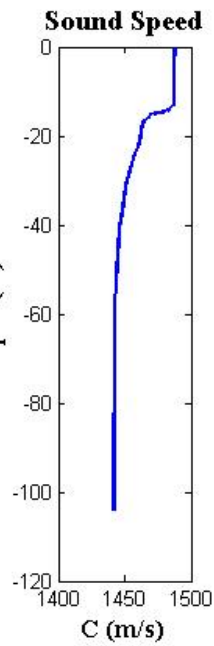
Ray tracing

West -> E Shore,

$\Delta\theta = 0.02$ deg



Brown Tower



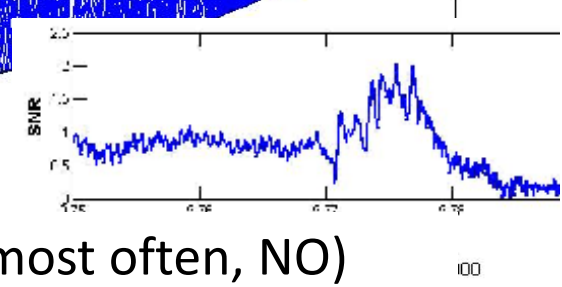
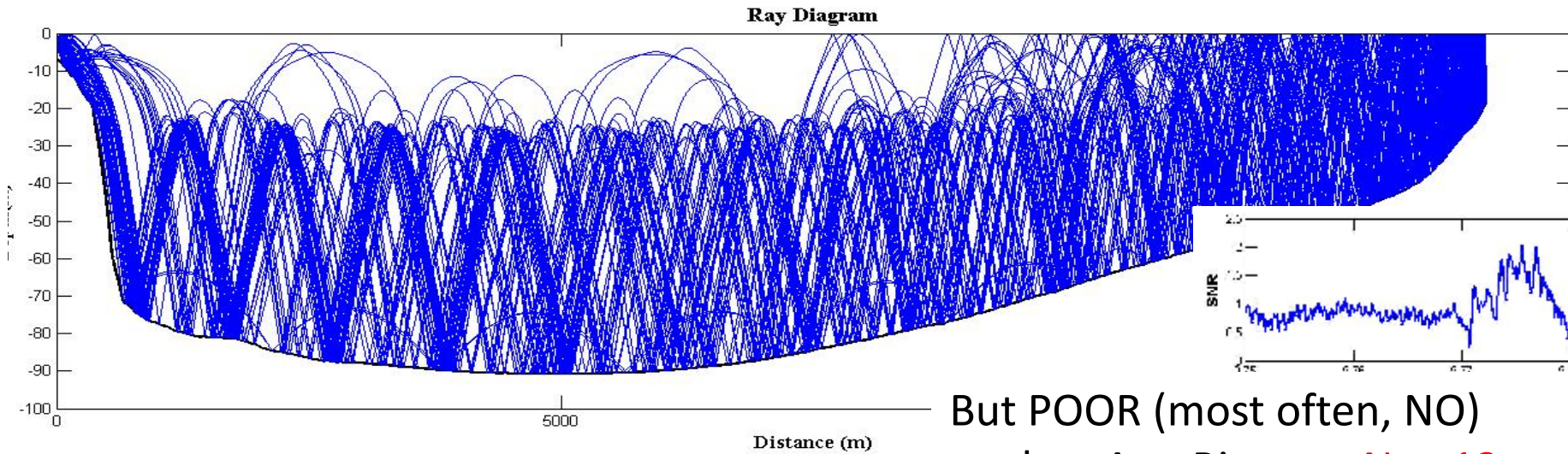
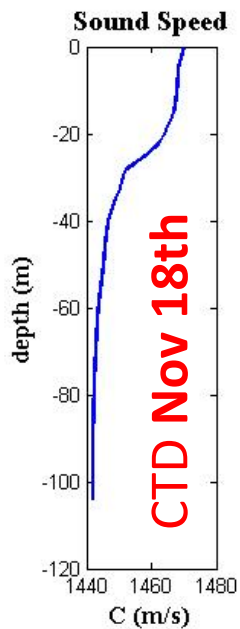
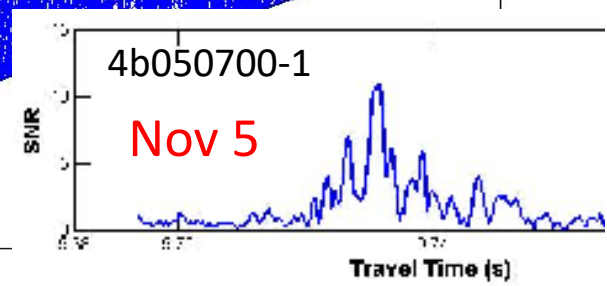
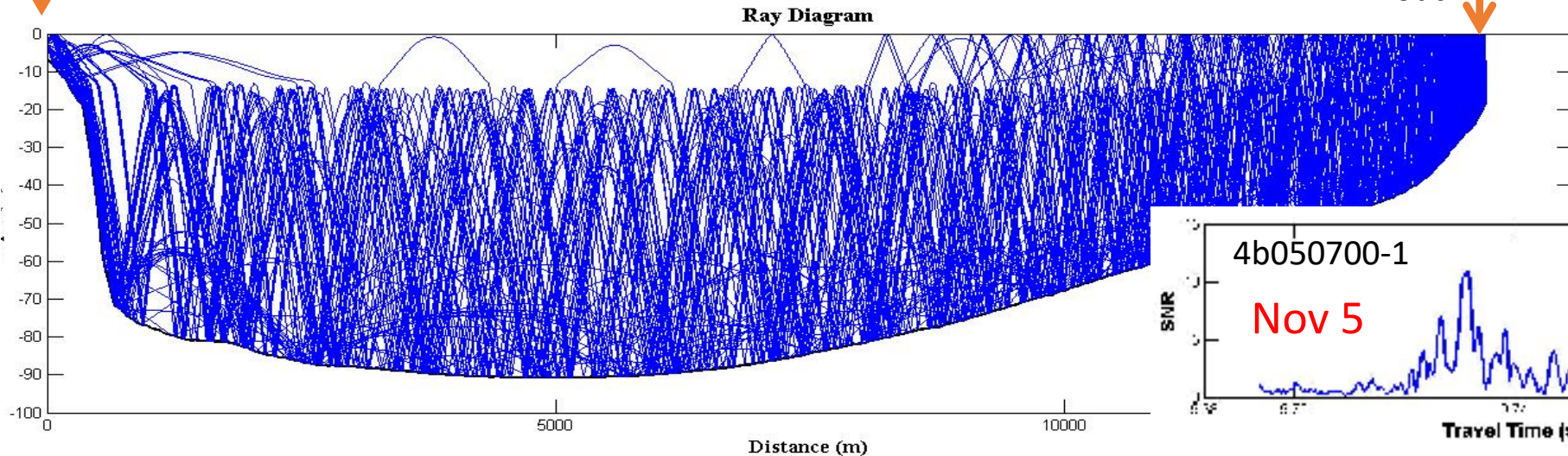
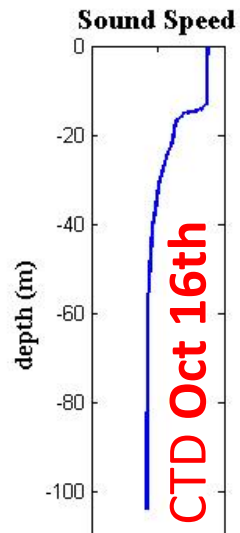
CTD Profile
from Oct 16th

Fairly stable reception
peak at Ane River (East
Shore) on Nov 5

Ray tracing West -> E Shore, $\Delta\theta = 0.02$ deg

Brown Tower
↓

nr Ane River mouth
↓

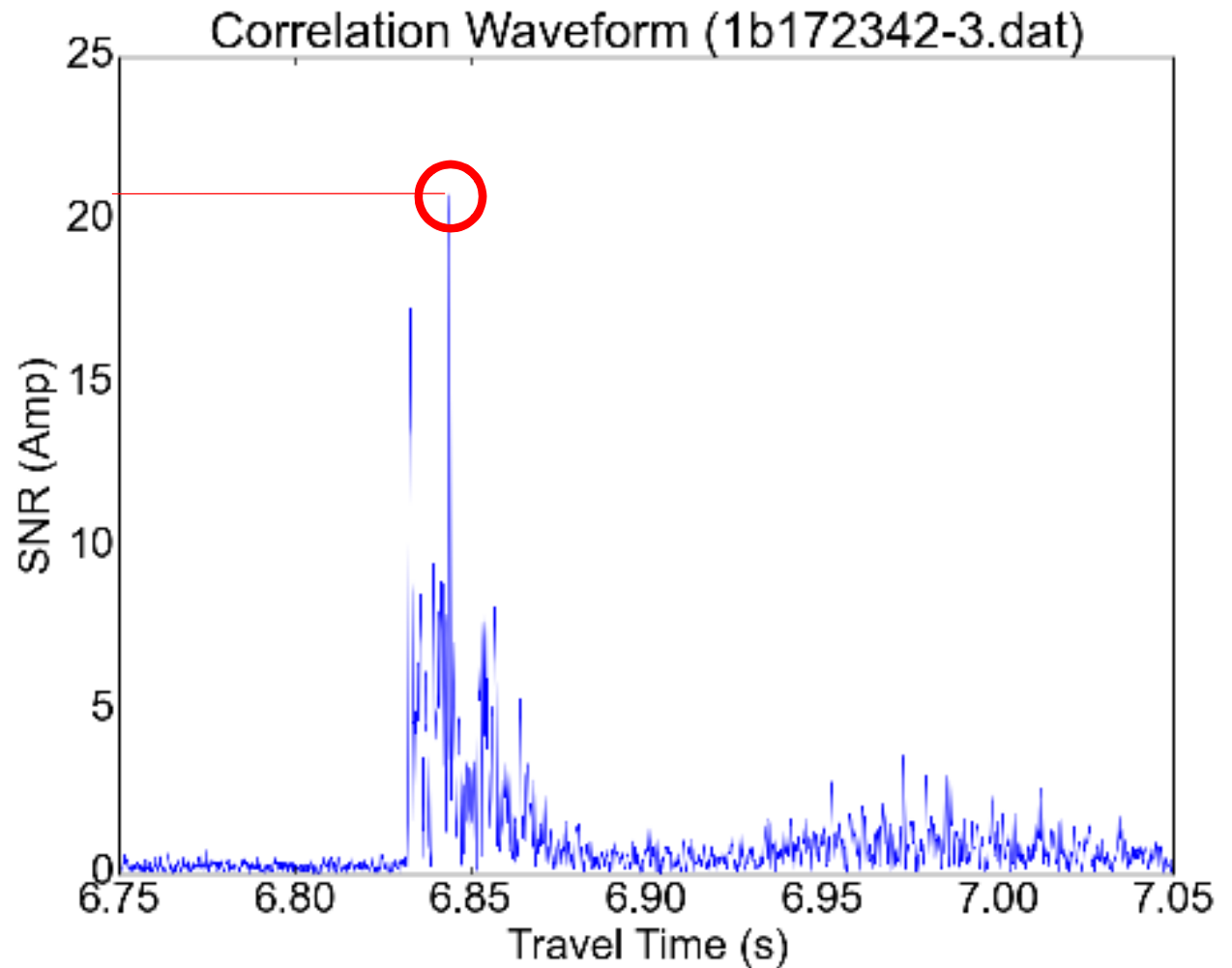


But POOR (most often, NO) peak at Ane River on Nov 13

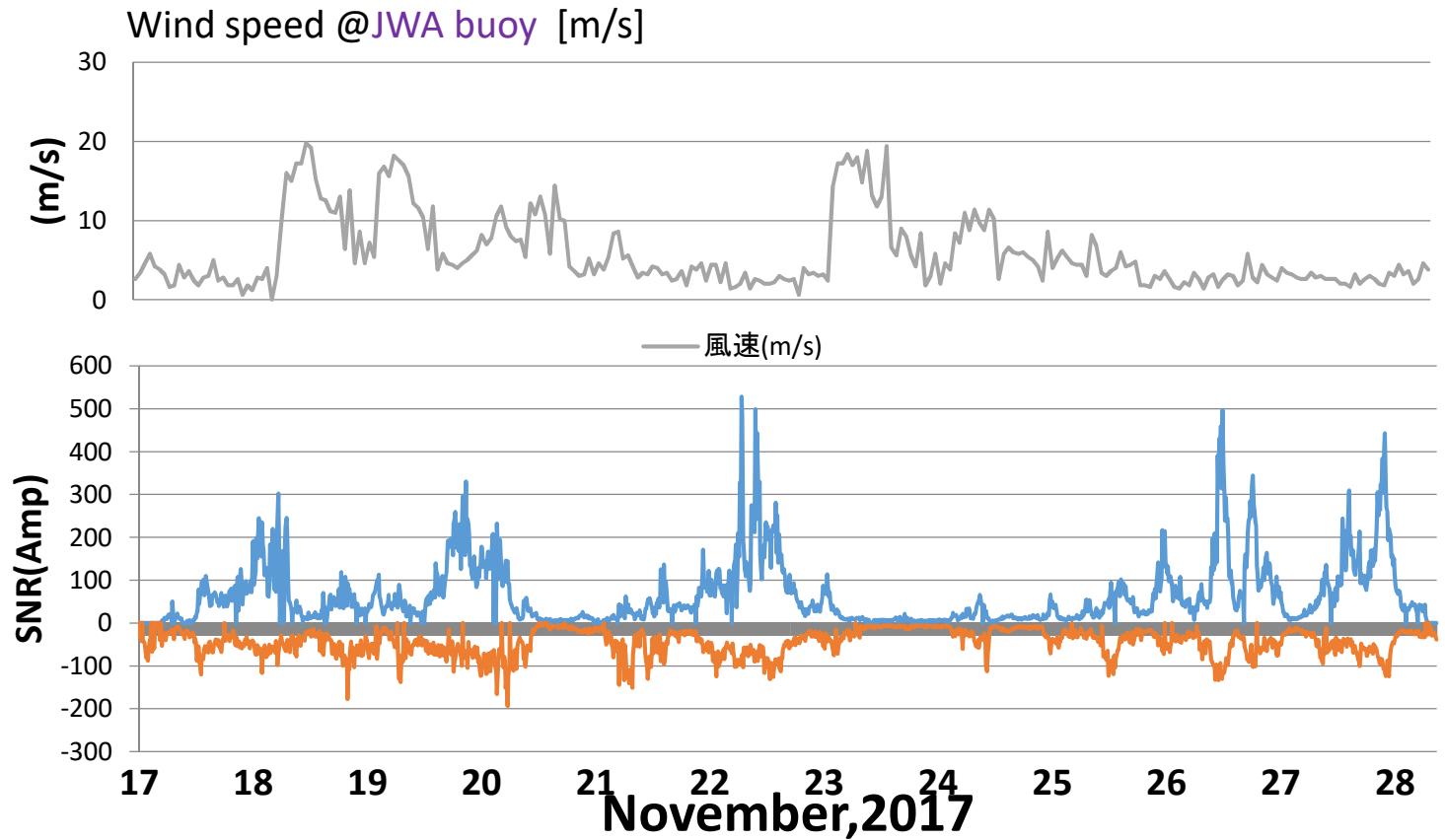
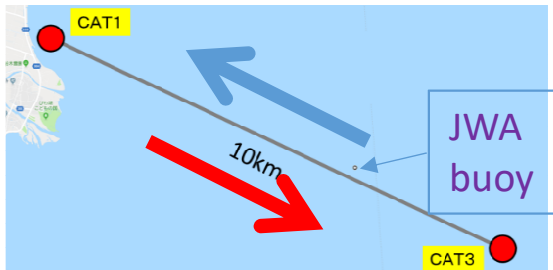
Nov. **2017**; after hardware upgrade w/ stronger emission,
“land-based” deployment @ Takeshima;
TR 2.5 m above Bottom@49 m. M11 * 6 repeats.



First, consider evolution of
Peak normalized correlation



evolution of peak normalized correlation

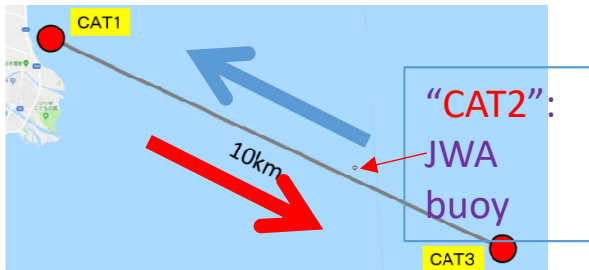


Rec'd CAT1 : +

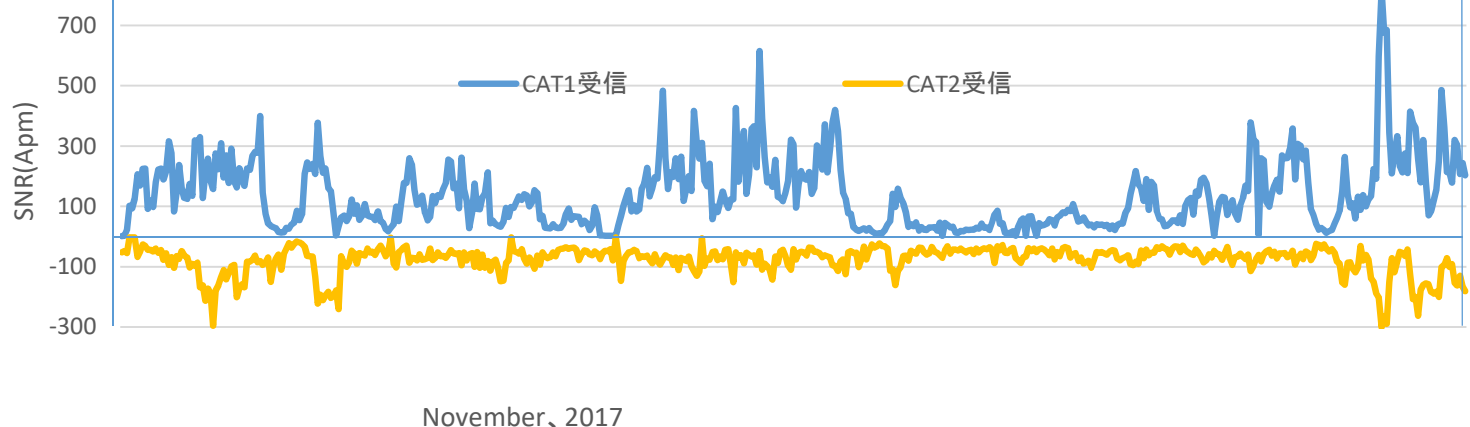
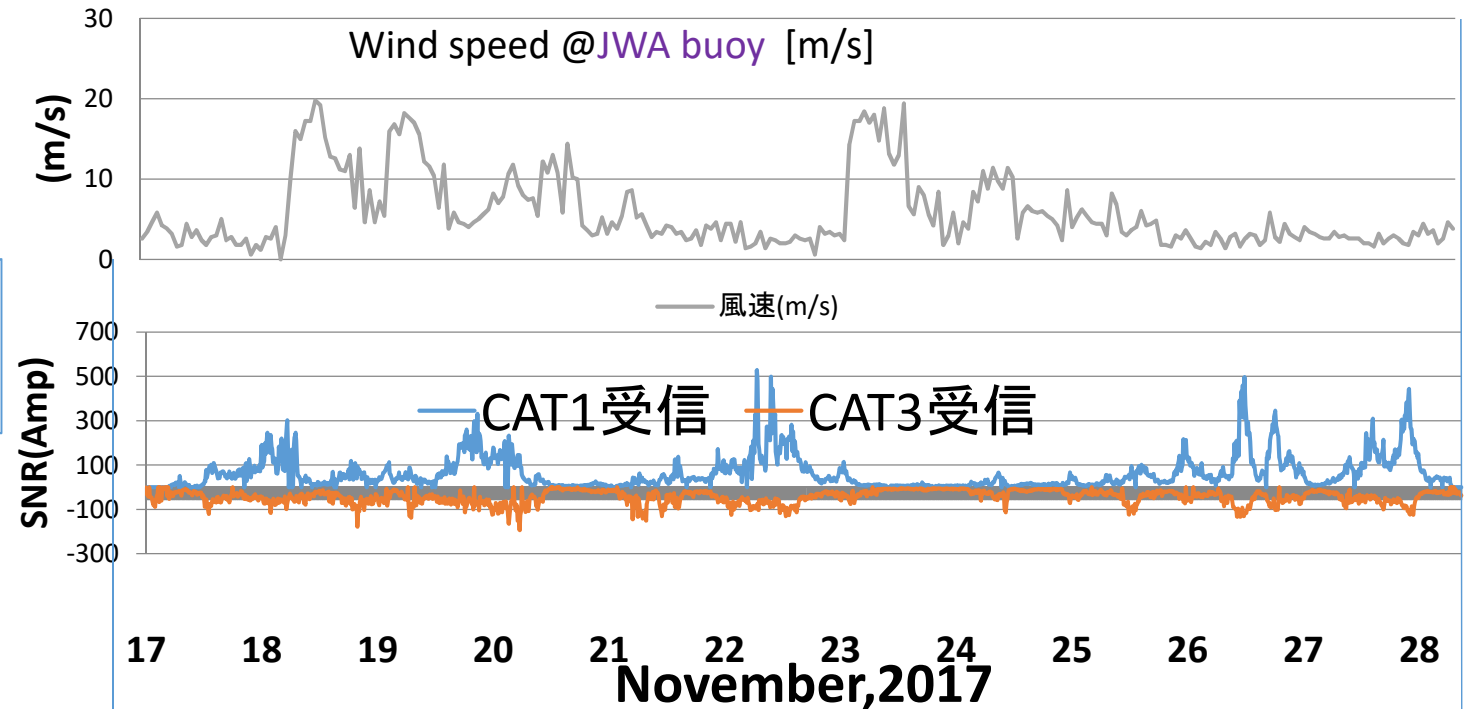
Rec'd CAT3 : - inverted plot

— CAT1受信 — CAT3受信

evolution of peak normalized correlation



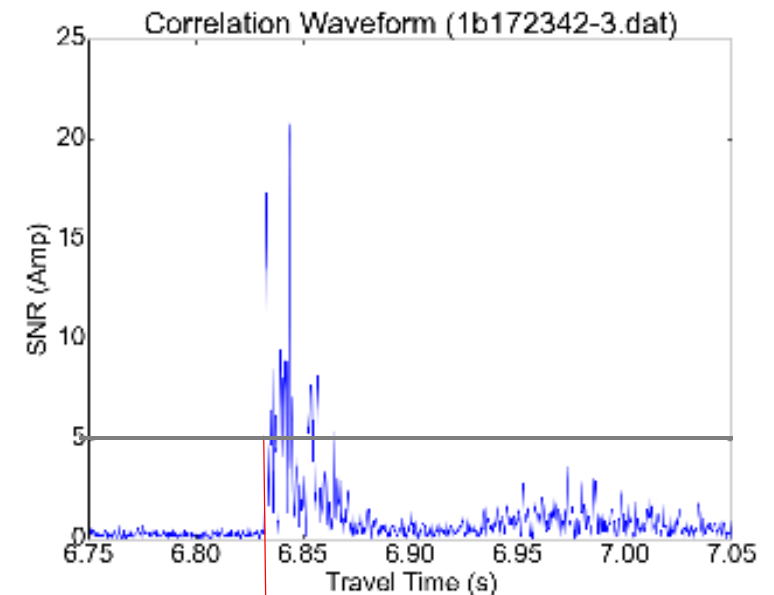
At $R = 10.2$ km, reception strength varies widely! Some intervals have rather low signal. This may explain inconsistent behavior at $R = 14.2$ km in Nov 2016



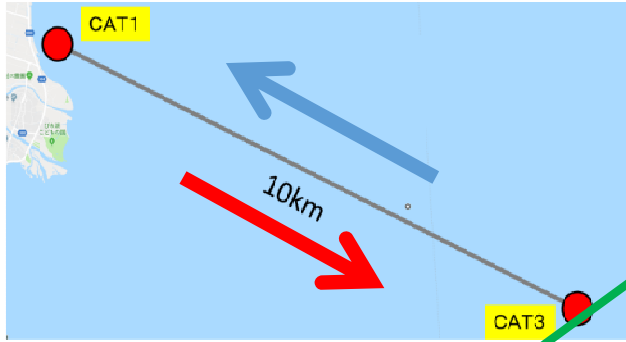
Note multiple peaks in correlogram!

Prof. C.F. Huang at NTU advised that we **characterize travel time by a threshold exceedance time**

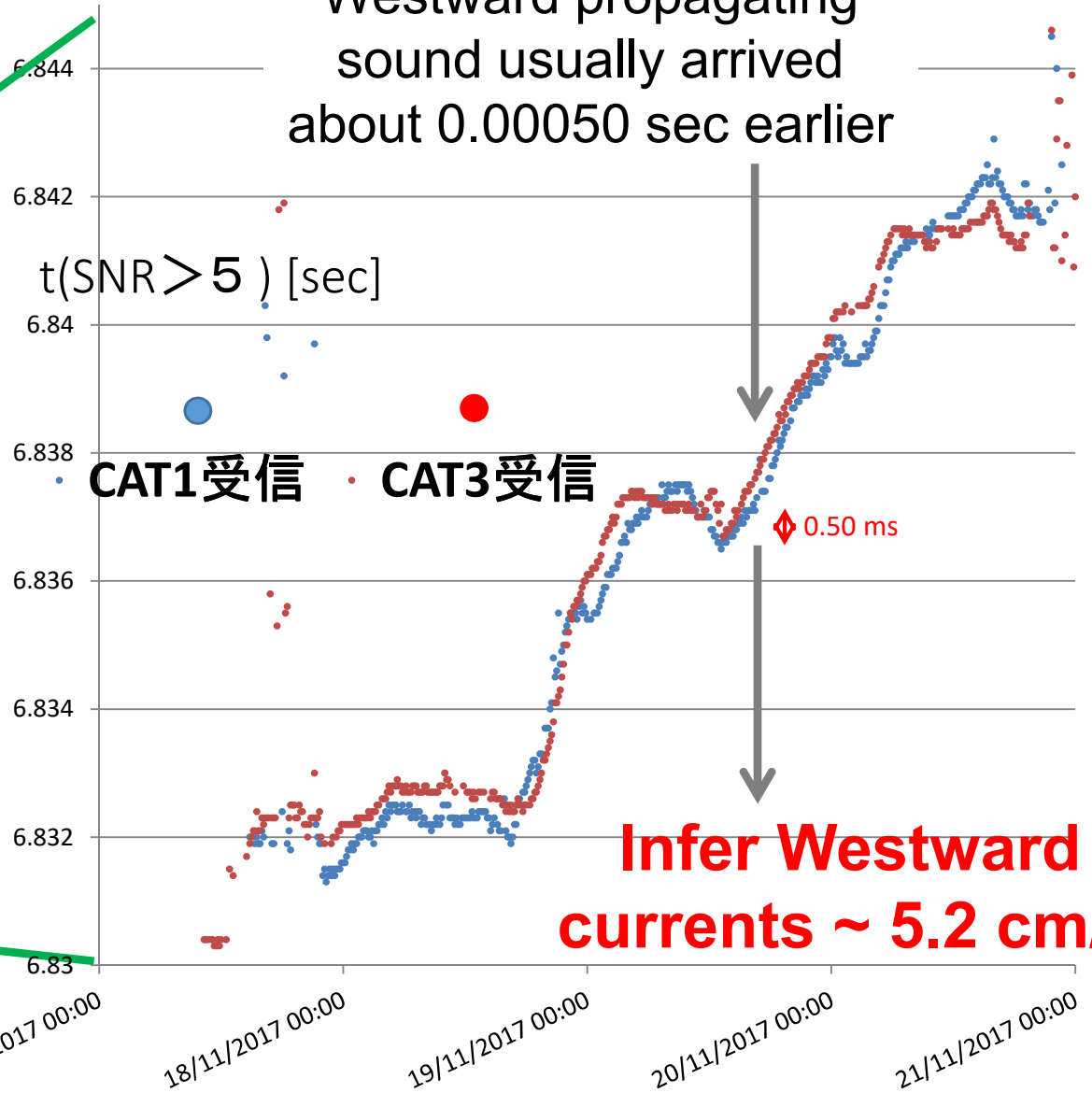
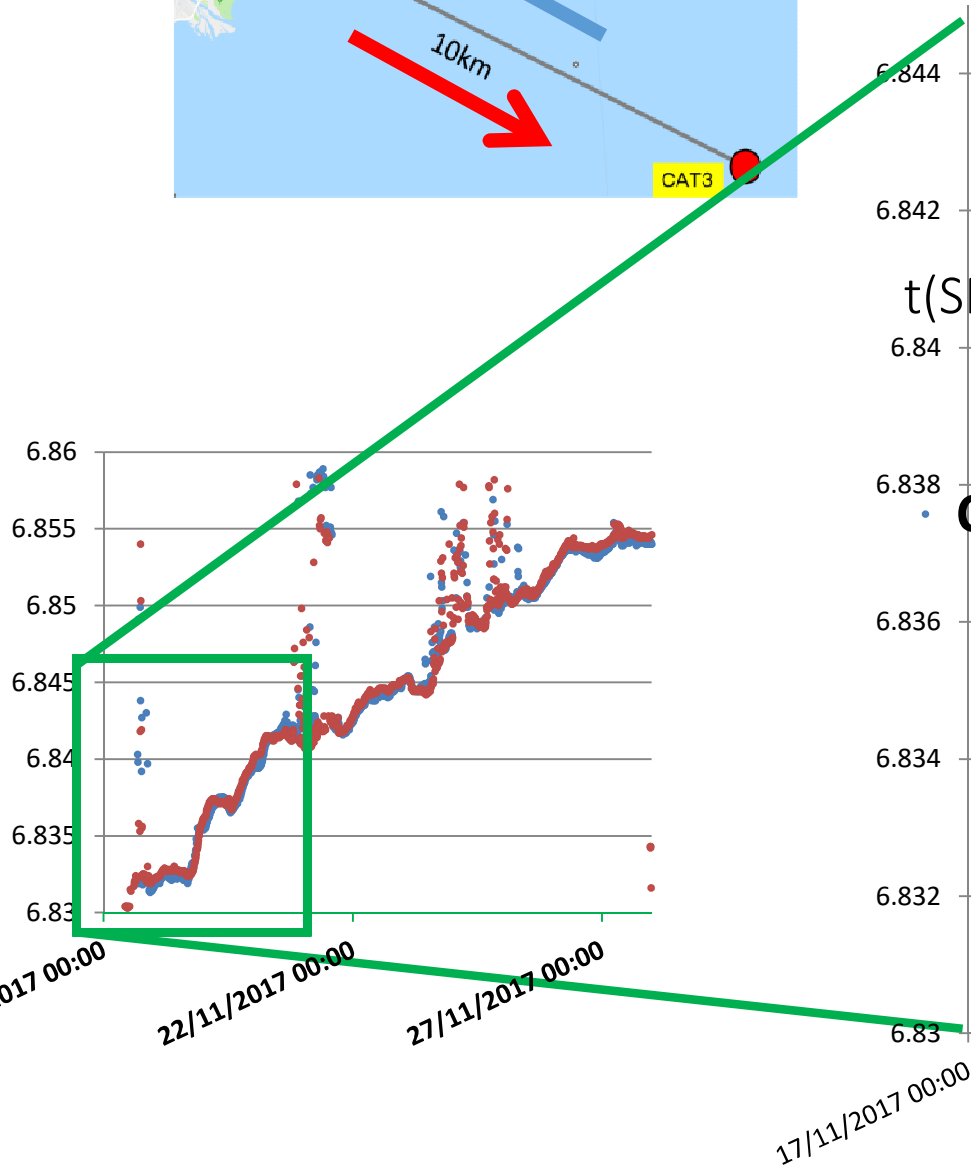
Next slide shows how this time evolved



$t_{\text{SNR}>5}$



Westward propagating sound usually arrived about 0.00050 sec earlier



Infer Westward currents ~ 5.2 cm/s

“Summary I.2” :With implementation of 6x repeat of M11, and further hardware upgrade, fairly consistent two way transmission has been achieved across the N Basin (R=10.2 km) under stratified conditions. **Small but consistent differences in travel times between reciprocal paths were observed, whence we estimate path-averaged currents along the dominant acoustic path on the order of 5 cm/s**, which is not inconsistent with expected magnitudes at this site. For the temperature profile in November, ray paths pass almost entirely below the thermocline. **To our knowledge this is the first reported estimate of currents by Acoustic Tomography in a lake.**

Next: Finer processing for Differential Travel Time, Comparison w/ hydro model + acoustic simulations (BELLHOP)

Longer term, will it be feasible to assimilate CAT results into an ocean model for L. Biwa?

RESEARCH ARTICLE

10.1002/2017JC012715

Key Points:

- Coastal acoustic tomography data were assimilated into a triangular mesh ocean model for the first time
- Velocities obtained from assimilation agreed with ADCP data better than those from inversion or simulation
- Assimilation with a triangular mesh fits complex coastlines well and enables reasonable circulation calculations

Correspondence to:

X.-H. Zhu,
xhzhu@sio.org.cn

Assimilation of coastal acoustic tomography data using an unstructured triangular grid ocean model for water with complex coastlines and islands

Ze-Nan Zhu^{1,2}, Xiao-Hua Zhu^{1,2} , Xinyu Guo³ , Xiaopeng Fan¹, and Chuangzheng Zhang¹ 

¹State Key Laboratory of Satellite Ocean Environment Dynamics, Second Institute of Oceanography, State Oceanic Administration, Hangzhou, China, ²Ocean College, Zhejiang University, Zhoushan, China, ³Center for Marine Environmental Study, Ehime University, Matsuyama, Japan

Abstract For the first time, we present the application of an unstructured triangular grid to the Finite-Volume Community Ocean Model using the ensemble Kalman filter scheme, to assimilate coastal acoustic tomography (CAT) data. The fine horizontal and vertical current field structures around the island inside the observation region were both reproduced well. The assimilated depth-averaged velocities had better agreement with the independent acoustic Doppler current profiler (ADCP) data than the velocities obtained by inversion and simulation. The root-mean-square difference (RMSD) between depth-averaged

Published online 1 SEP 2017

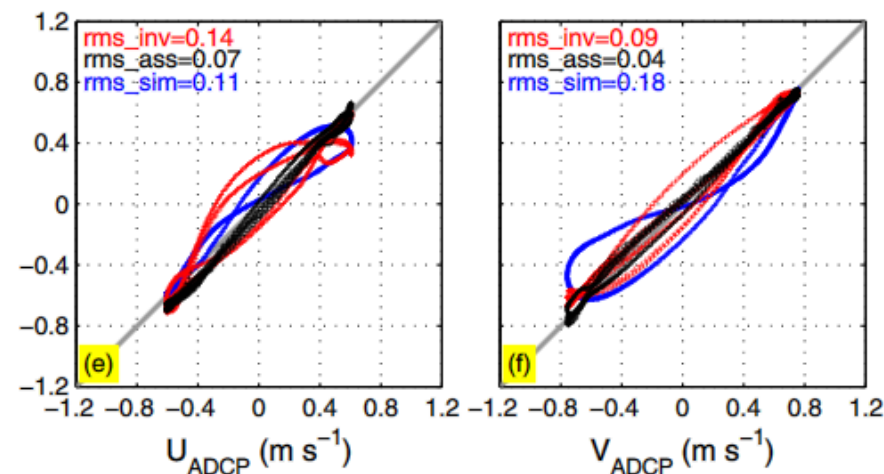
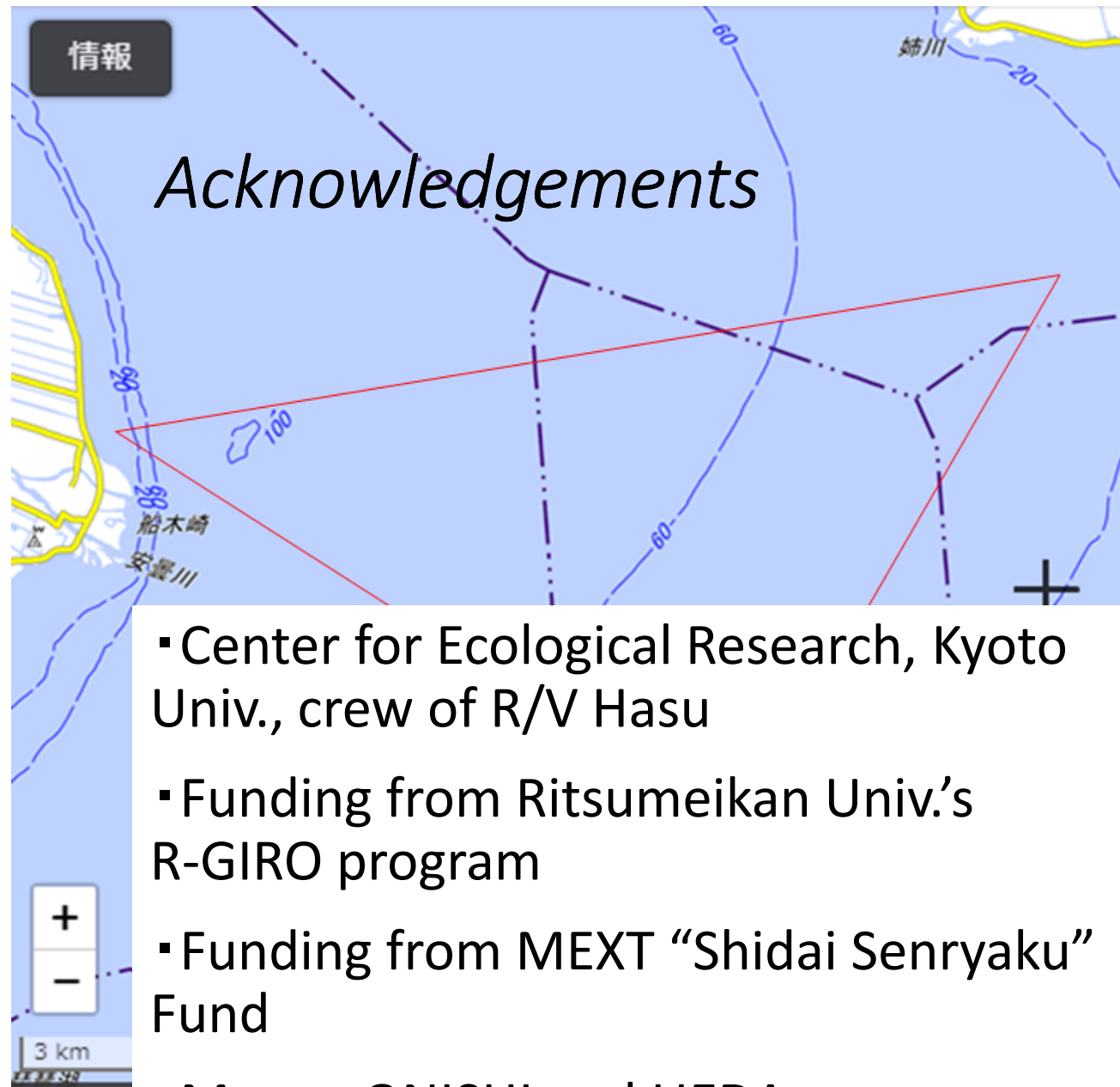


Figure 7. Scatter plots of (left) eastward and (right) northward velocity components with respect to ADCP at stations (top) A1, (middle) A2, and (bottom) A3. The RMSDs between the ADCP and the inversion, assimilation, and simulation are shown in the top left of each figure (in $m s^{-1}$).

“Plans for a followup three-month test scheduled to start in late **August** 2018 will be presented. We solicit suggestions for designing this and future tests to **best contribute to understanding of Continental-Coastal Ocean interactions.**”

L Biwa is a well-documented, well instrumented/sampled tide-free “test bed” for comparative research!

Topographic effects,
Orographic effects,
Lovely internal waves/seiches,
“World’s most beautiful”
lacustrine gyre...

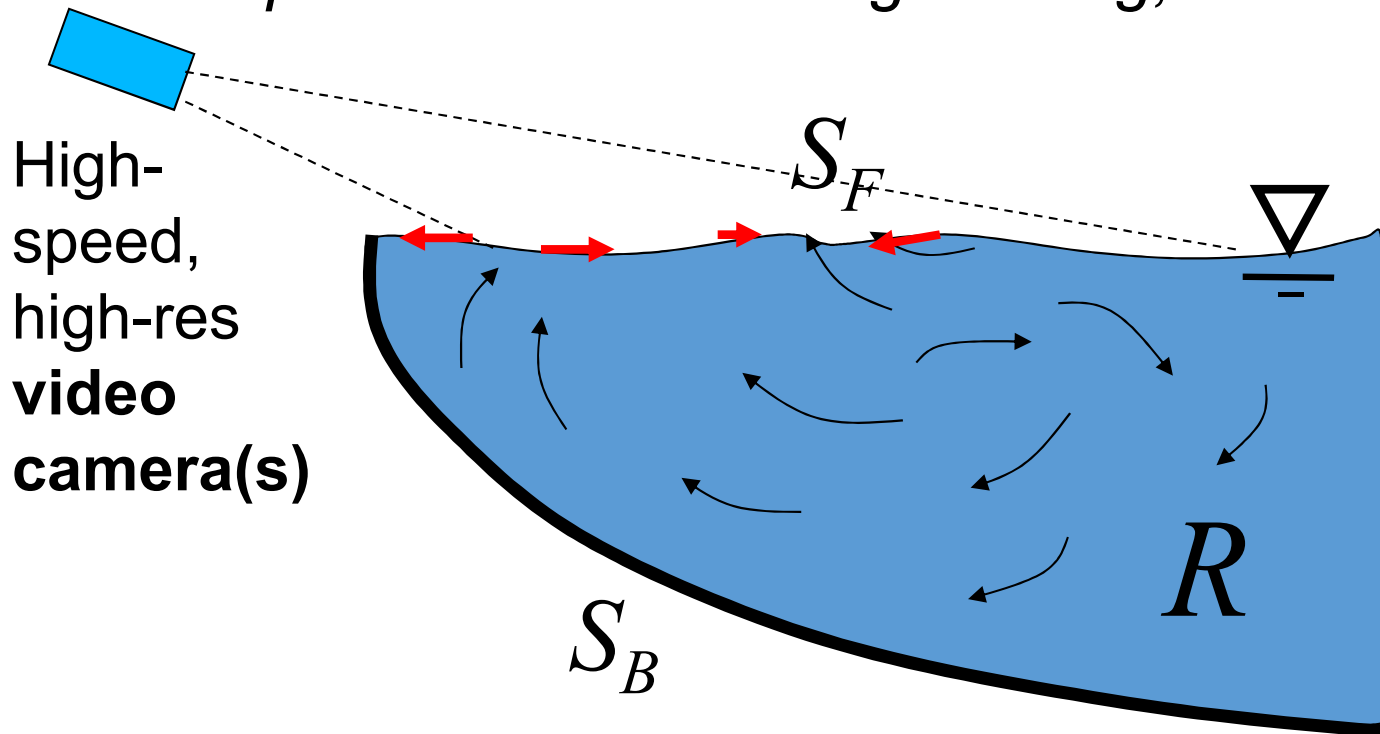


- Center for Ecological Research, Kyoto Univ., crew of R/V Hasu
- Funding from Ritsumeikan Univ.’s R-GIRO program
- Funding from MEXT “Shidai Senryaku” Fund
- Messrs ONISHI and UEDA, Ritsumeikan undergrads

Part II: RELATIONS BETWEEN QUANTITIES AT A WATER SURFACE WITH THE INSTANTANEOUS SUBSURFACE FLOWFIELD

•J.C. Wells

•*Department of Civil Engineering, Ritsumeikan University*



Overall Motivation:

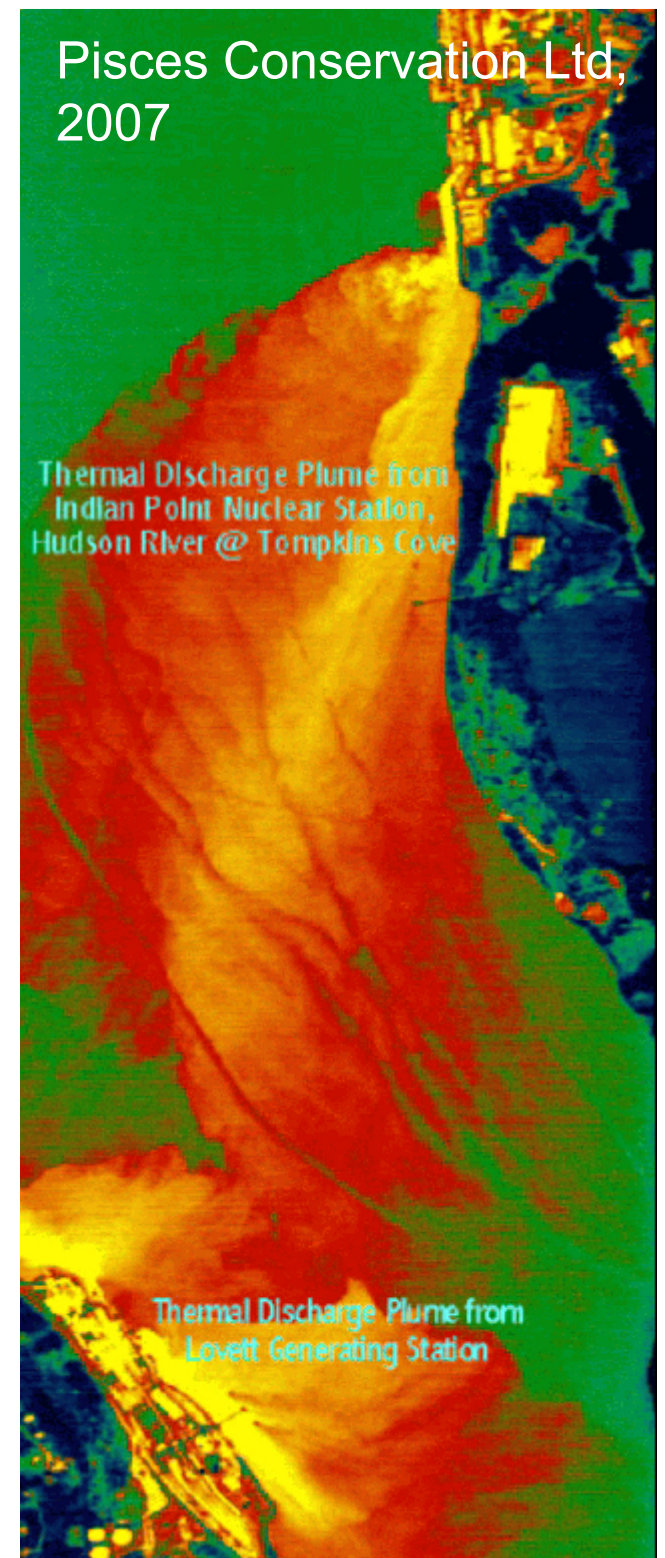
Measurement models for
“nowcasting” of flowfields,

e.g. river/estuary flowfields (thence
thermal impacts, pollutant
dispersion, *etc.*)

Pisces Conservation Ltd,
2007

Thermal Discharge Plume from
Indian Point Nuclear Station,
Hudson River @ Tompkins Cove

Thermal Discharge Plume from
Lovett Generating Station



First, review our prior *empirical*
estimation
(stochastic estimation)

POD-BASED ESTIMATION OF THE FLOW FIELD FROM FREE-SURFACE VELOCITY IN THE BACKWARD-FACING STEP

T. NGUYEN¹, T. DINH¹, J. WELLS¹, P. MOKHASI², D. REMPFER³

¹ Ritsumeikan University, Japan

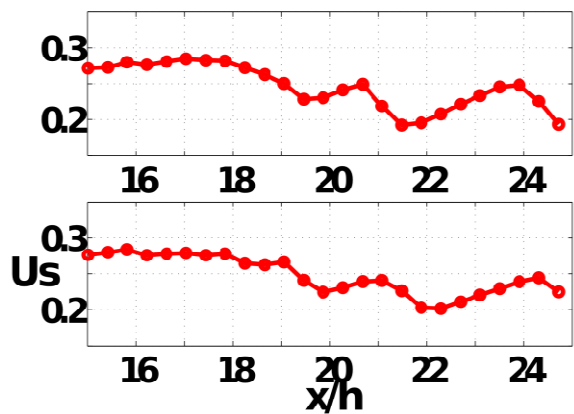
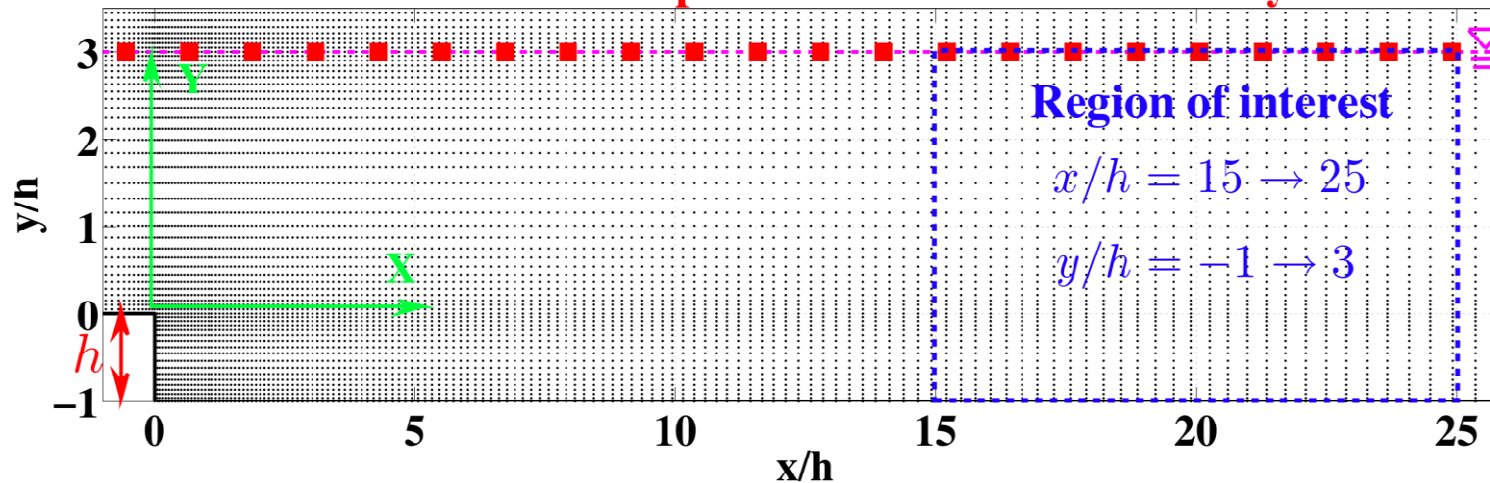
² Wolfram Research Inc., Illinois

³ Mechanical, Materials & Aerospace Engineering, Illinois Inst. Technology

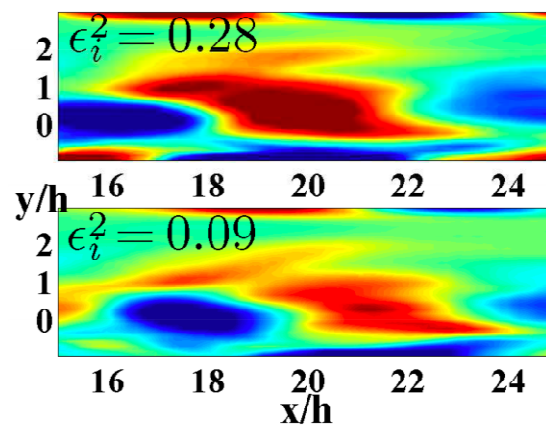
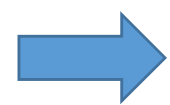
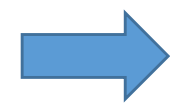
TSFP-7

Ottawa, July 30 2011

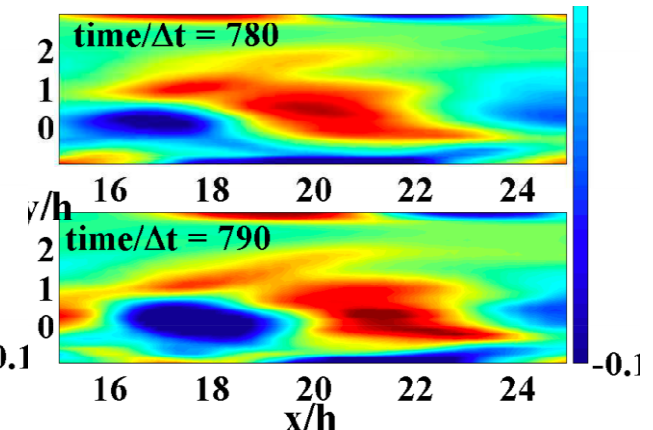
Measurement points of free-surface velocity



$U(x)@surface$



ω_z (regression model)



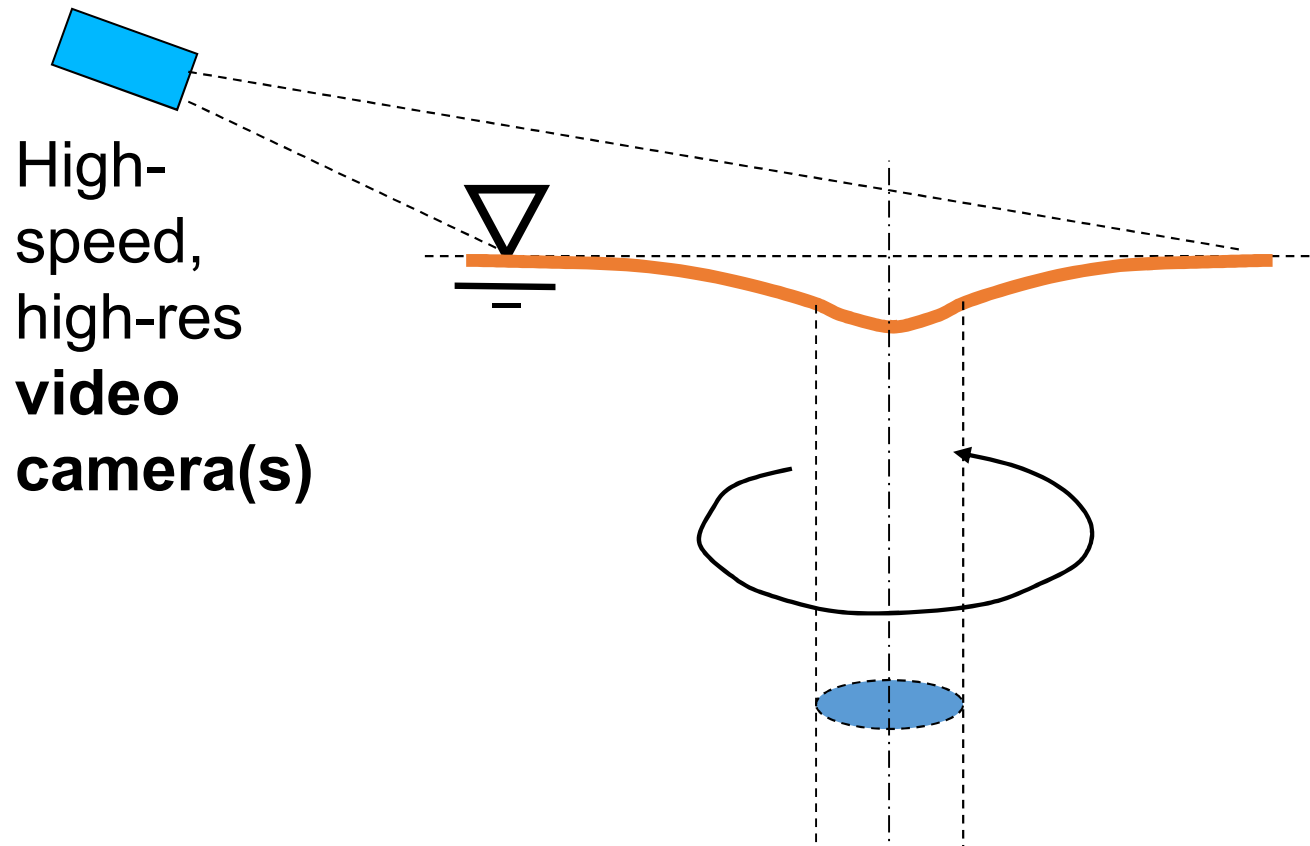
ω_z from LES

“PIV” citation: Nguyen, T.D., J. Wells, P. Mokhasi, and D. Rempfer (2010) “POD-based estimations of the flow field from particle image velocimetry wall-gradient measurements in the backward-facing step flow,” *Meas. Sci. Technol.*, vol. 21(11) 1–15

INTEGRAL RELATIONS, KINEMATIC AND DYNAMIC, BETWEEN THE FLOW AT A LIQUID SURFACE AND THE SUBSURFACE FLOWFIELD

John C. Wells

•Dept. Civil Engineering, Ritsumeikan University, Japan



1 SCENARIO: LOCAL REMOTE SENSING OF A RIVER SURFACE,

- Measurements of **surface velocity** (+water level) from (stereo) **video recording** continues to progress.
- With this motivation, I **theoretically discuss the possibilities for estimating subsurface flow from the fluctuating velocities and fluctuating height at the water surface**

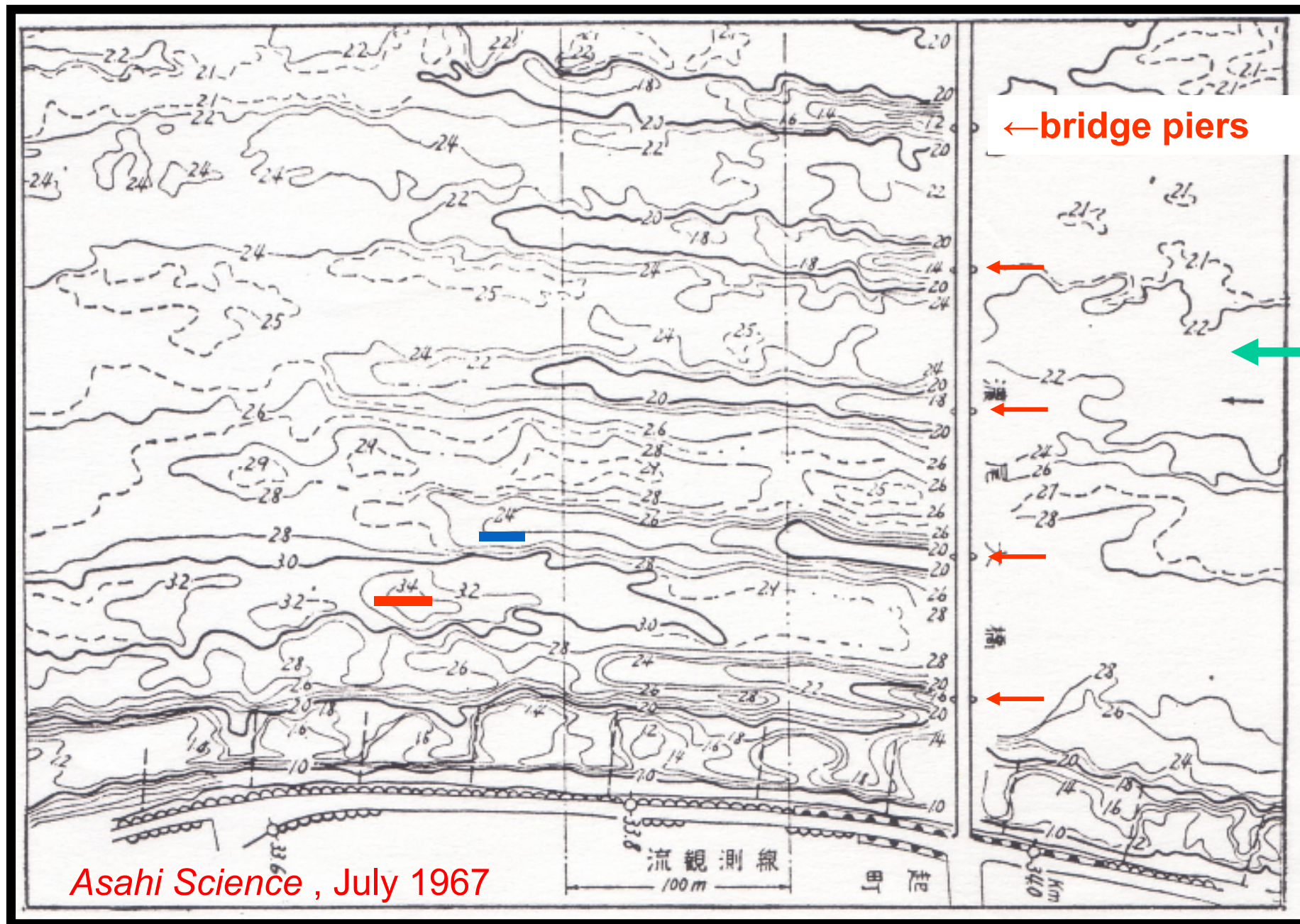
SOME PRIOR LITERATURE ON REMOTE SENSING OF A RIVER SURFACE

“Aerial PIV” by Dr. R. Kinoshita



1988 (63 yrs)

Analysis of flood flows; resistance of bridge



主流

← bridge piers

Asahi Science, July 1967

(Bank-mounted) “Large Scale” PIV

- Prof. I Fujita, Kobe University (started with Iowa group)
 - Chikadel & Jessup, APL, U. Washington (using IR)

Zhang X.,
Dabiri D.,
& Gharib M., 1994

“A Novel Technique
For Free-Surface
Elevation Mapping,”
Physics of Fluids **6** (9)

(and Lisbon Conf.
on Laser
Techniques in Fluid
Meas't, 1993)

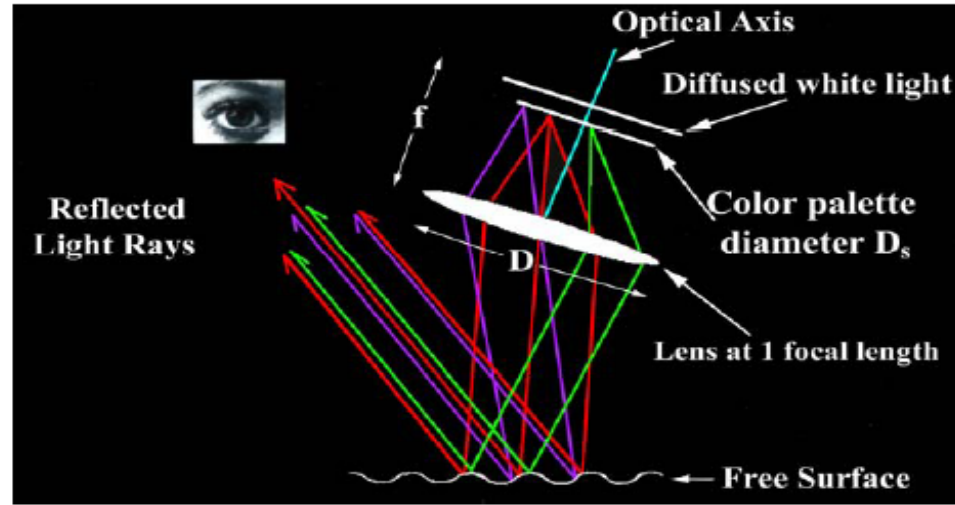
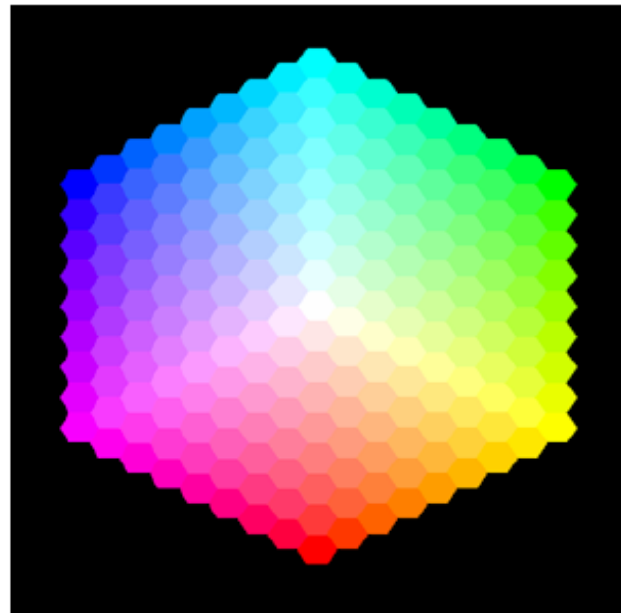


Fig. 1 This picture demonstrates the principle of the measurement technique. A diffused white light source illuminates a color palette (see Fig. 2). A lens, located at its focal plane from the color palette, transforms the merging color-coded light into a multiple system of parallel colored beams. This system of beams, after being reflected from the free-surface, is captured by a camera located far away. It is important to note that each color will reflect from a particular slope of the free-surface. Thus, the basis of the technique lies in the fact that different slopes of the free-surface are coded with different colors, through the setup of the color palette and lens as explained above.



Zhang, Dabiri, Gharib, 1994

Imaged area= 22*15 cm

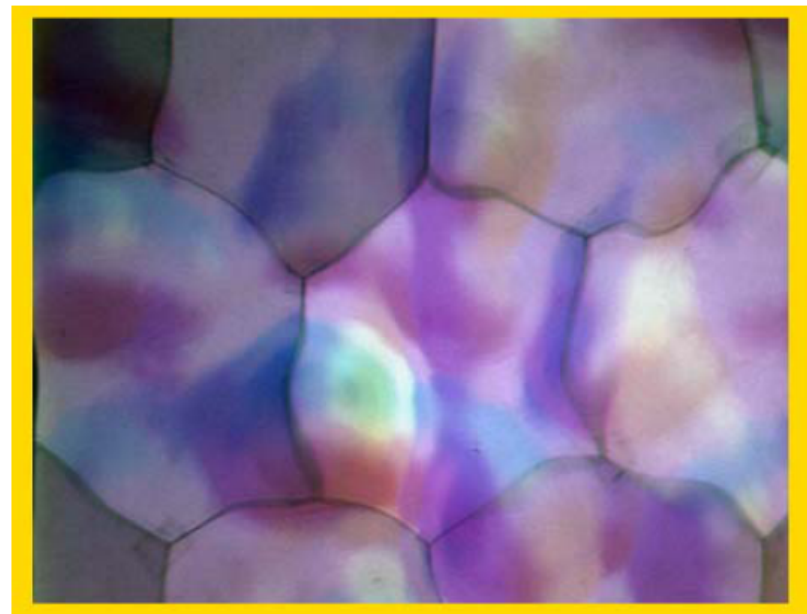


Fig. 5 A picture of the free-surface captured by a RGB color video camera. The surface is deformed by the turbulence generated within the volume of the fluid. The images covers an area of 22 cm by 15 cm. Again, it is necessary to emphasize that this picture and picture 8 are real, and are not pseudo-colored.

~ 0.05 mm accuracy!,
nearly 20 years ago.

(BUT lab experiment,
small field of view)

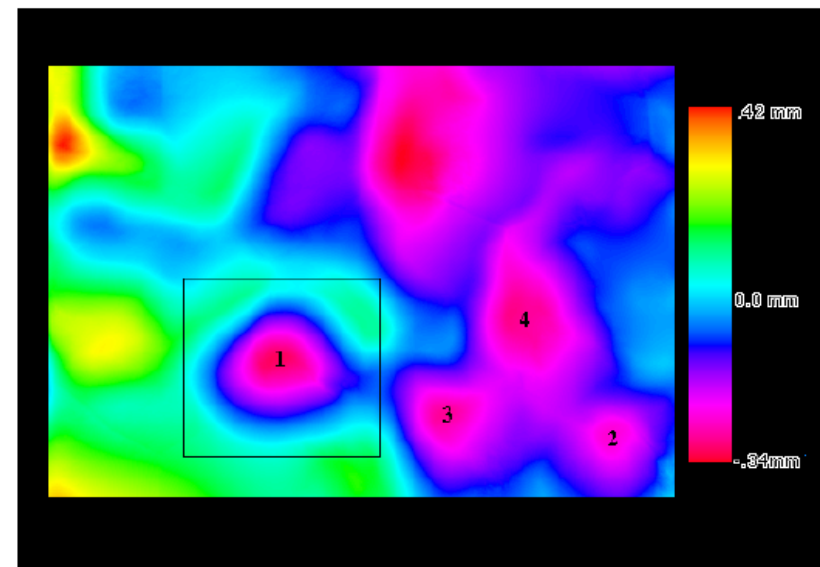


Fig. 7 Surface elevations calculated from the measured slopes extracted from picture 5. The surface elevation ranges from -0.34 mm to 0.42 mm. Note that there are several circular depressions within the free-surface indicating vortex connections to the free-surface.

SOME PRIOR LITERATURE ON ESTIMATING SUBSURFACE FLOW FROM REMOTE SENSED SURFACE INFORMATION

- Estimates of flow near the **sun's surface**;

Alain Vincent et al. (2006) used magnetic flux at surface (coupled with flow by MHD) to estimate the flow field of plasma

- I have so far failed to find similar data assimilation in “terrestrial” hydrodynamics. I **solicit relevant citations!**

Relations between **surface** and **subsurface quantities**;

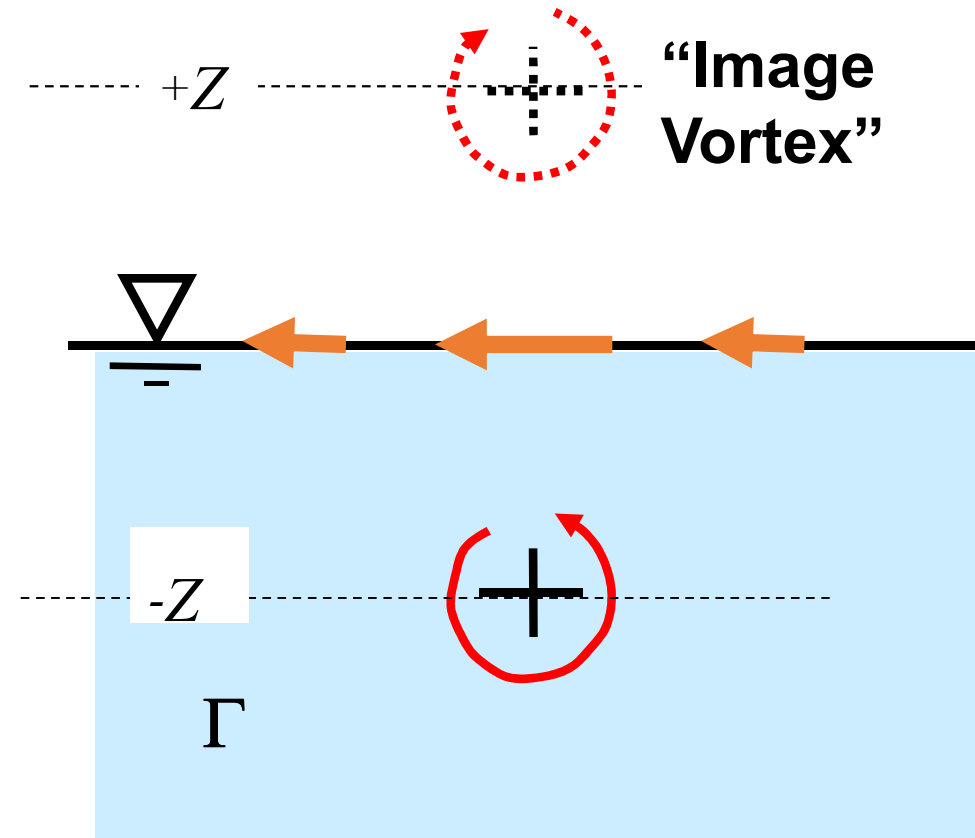
•2 **KINEMATIC RELATIONS**

• 2.1 Biot-Savart + Image Vortices

• 2.2 Integral Relation

•3 **DYNAMIC RELATION**

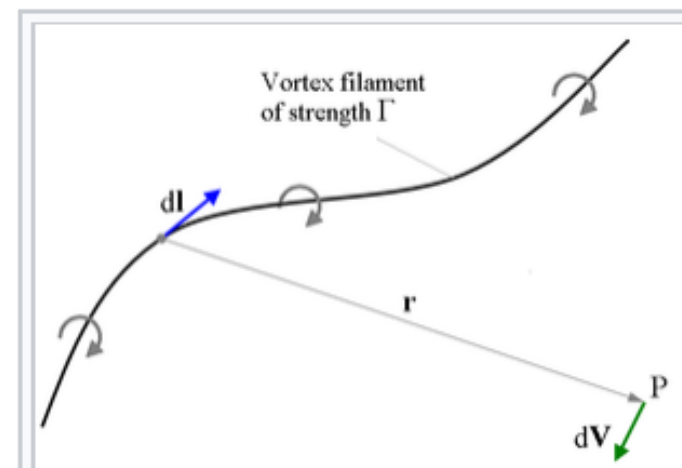
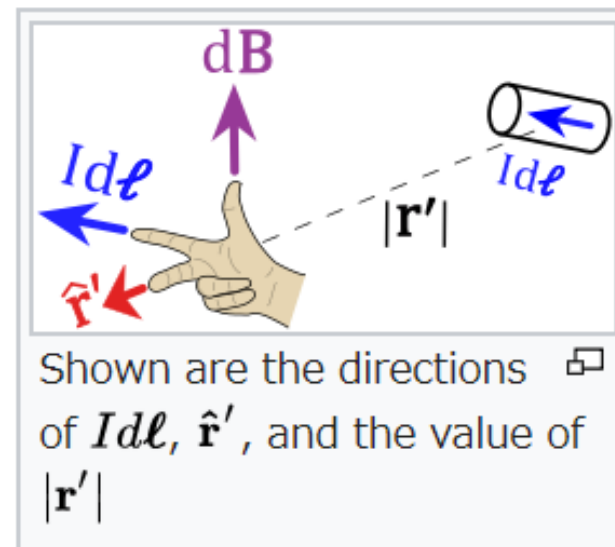
• Integral Relation between total head at surface with subsurface “vortex force”



The Biot–Savart law is used for computing the resultant **magnetic field** \mathbf{B} at position \mathbf{r} in 3D-space generated by a *steady current* I (for example due to a wire). A steady (or stationary) current is a continual flow of **charges** which does not change with time and the charge neither accumulates nor depletes at any point. The law is a physical example of a **line integral**, being evaluated over the path C in which the electric currents flow (e.g. the wire). The equation in **SI units** is^[3]

$$\mathbf{B}(\mathbf{r}) = \frac{\mu_0}{4\pi} \int_C \frac{I d\boldsymbol{\ell} \times \mathbf{r}'}{|\mathbf{r}'|^3}$$

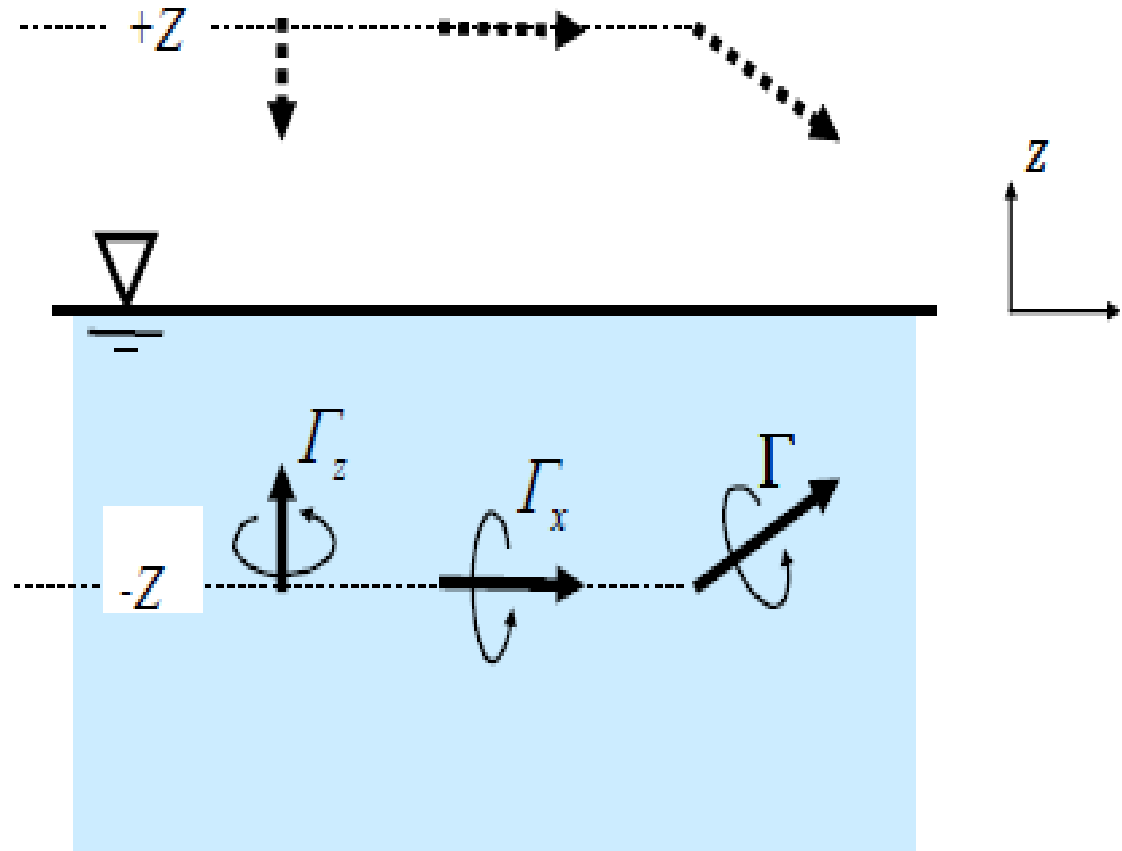
en.wikipedia.org/wiki/Biot-Savart_law



The figure shows the velocity ($d\mathbf{V}$) induced at a point P by an element of vortex filament ($d\mathbf{L}$) of strength Γ .

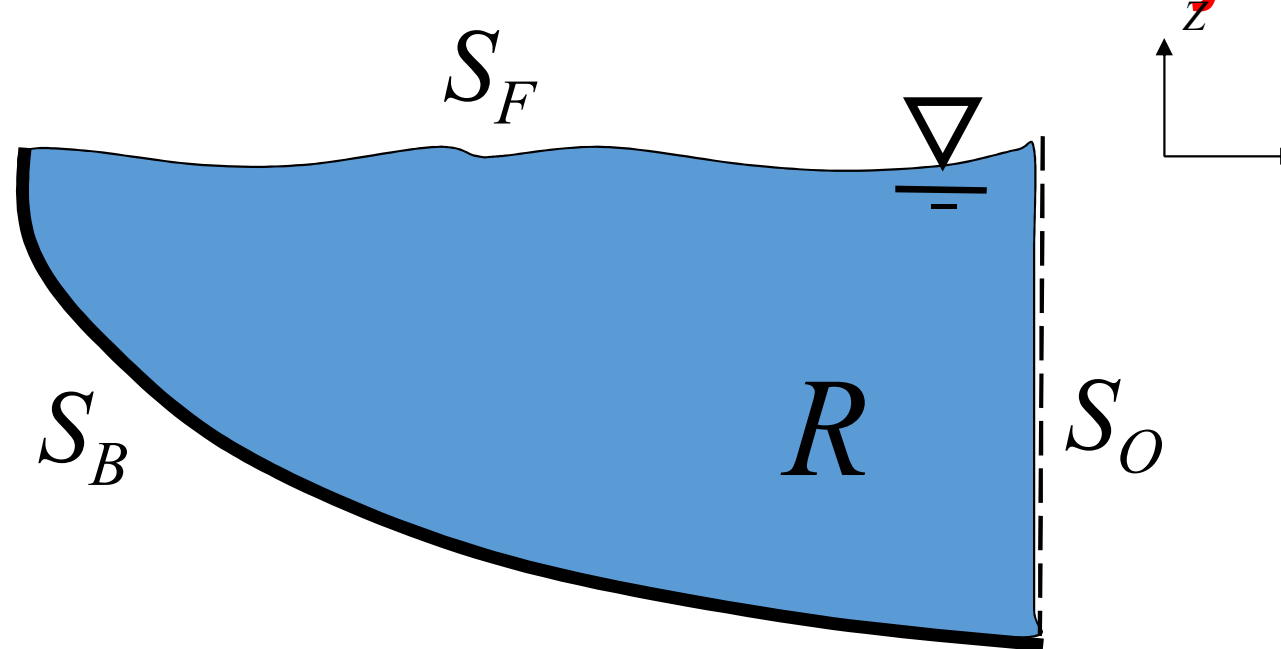
2 KINEMATIC RELATIONS

•2.1 “Classical”: Biot-Savart + Image Vortices



→ Only valid for VERY simple geometries...

2. An Integral Relation between **surface velocities** and **subsurface vorticity**

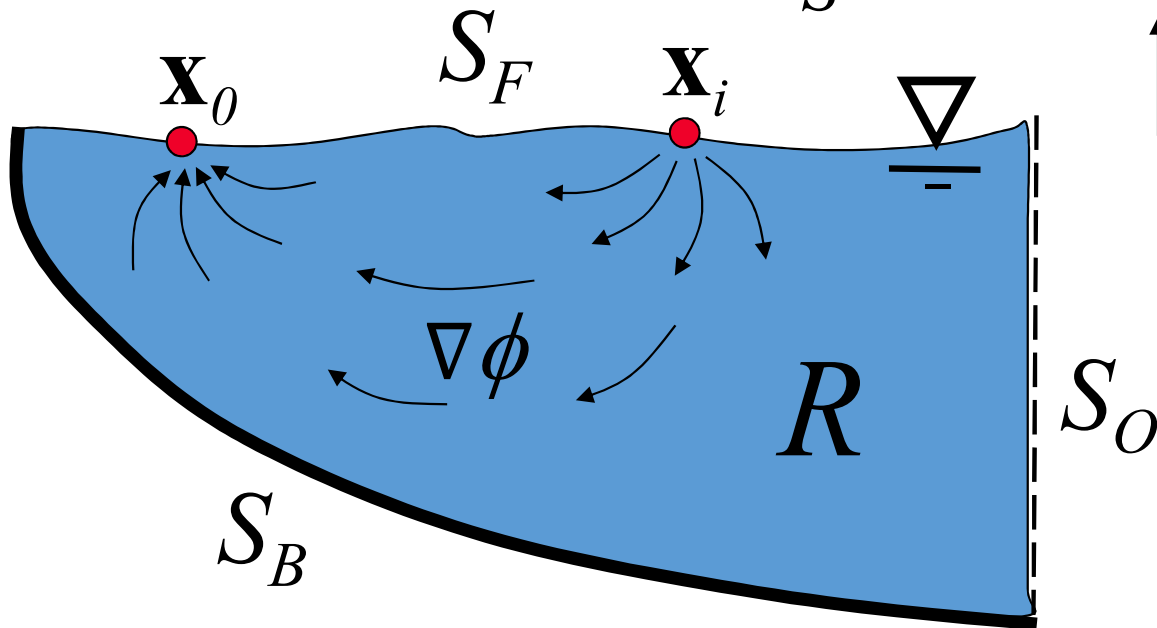


integrating $\int_R \boldsymbol{\omega} \times \nabla \phi dV$ by parts, invoking $\nabla \cdot \mathbf{u} = 0$
and $\boldsymbol{\omega} = \nabla \times \mathbf{u}$, applying the divergence theorem;

$$\int_R \boldsymbol{\omega} \times \nabla \phi dV = \int_S (\mathbf{u} \nabla \phi - \phi \nabla \mathbf{u}) \cdot \mathbf{n} dS$$

cf. Biot-Savart

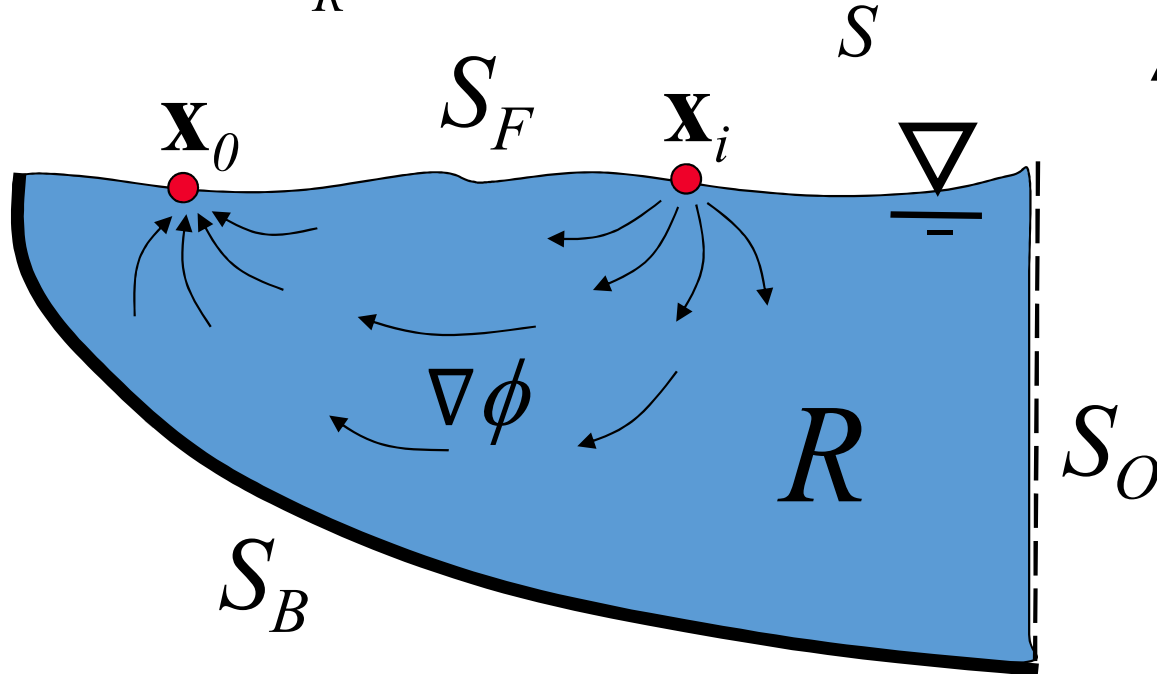
$$\int_R \boldsymbol{\omega} \times \nabla \phi dV = \int_S (\mathbf{u} \nabla \phi - \phi \nabla \mathbf{u}) \cdot \mathbf{n} dS$$



We can choose ϕ to “extract” surface velocities (from RHS) at just two points, by specifying $\nabla \phi \cdot \mathbf{n} = 0$ on S , everywhere except for a point sink at \mathbf{x}_0 and a point source \mathbf{x}_i .

Then fixing \mathbf{x}_0 and “scanning” \mathbf{x}_i over N points on the surface would yield a system of $3N$ weighted integrals of (unknown) subsurface vorticity .

$$\int_R \boldsymbol{\omega} \times \nabla \phi dV = \int_S (\mathbf{u} \nabla \phi - \phi \nabla \mathbf{u}) \cdot \mathbf{n} dS$$



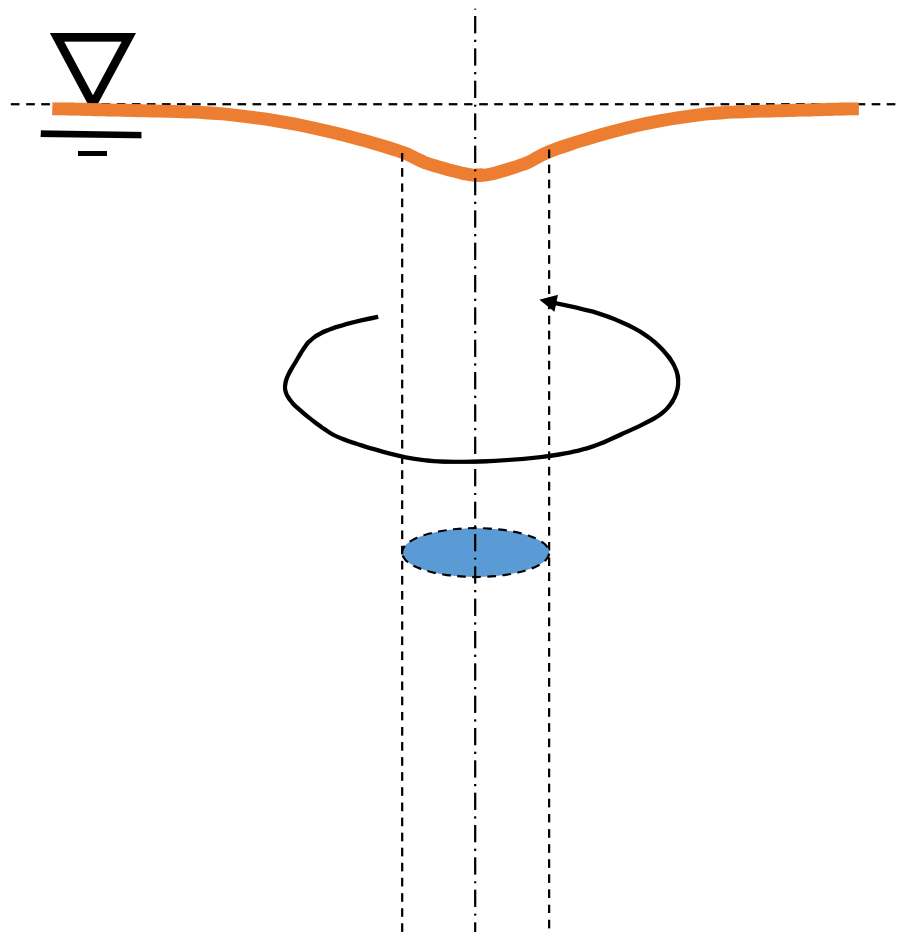
...yields a linear system of $3N$ equations for $3M$ unknowns (vorticity at $m=1,2,\dots,M$).

RECALL, HOWEVER, the nonunique relation between a vortex and surrounding velocity; cf. Hill's spherical vortex.

→ Interpret this equation as a “constraint”

3. DYNAMIC RELATION

Integral Relation between total head at surface with subsurface distribution of “vortex force”



3. DYNAMIC RELATION: Integral Relation between **total head at surface** with subsurface distribution of **“vortex force” (Lamb vector)**.

Now **start from Euler Equation** (though viscosity can be handled);

$$\frac{\partial \mathbf{u}}{\partial t} = (\mathbf{u} \times \boldsymbol{\omega}) - \nabla \left(\frac{u^2}{2} + \frac{p}{\rho} + gz \right) = \underline{(\mathbf{u} \times \boldsymbol{\omega})} - \nabla (g\underline{E})$$

Applying Divergence Theorem, etc, and with the same choice of analyzing function as before;

$$\frac{1}{\rho} \underline{(E(\mathbf{x}_i) - E(\mathbf{x}_0))} = \int_R \underline{(\mathbf{u} \times \boldsymbol{\omega})} \cdot \nabla \psi dV + \int_S \psi \frac{\partial \mathbf{u}}{\partial t} \cdot \mathbf{n} dS$$

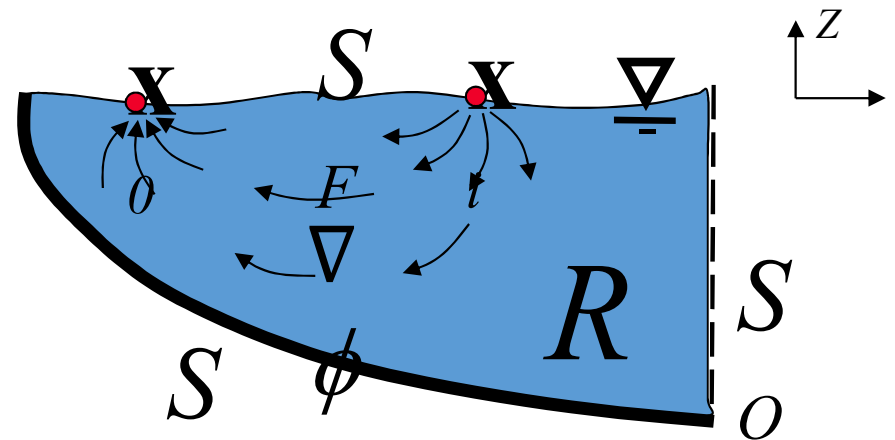
Numerically **TEST INVERSION** of Integral Relation between **total head at surface** with subsurface distribution of “**vortex force**” (Lamb vector).

Measure this,

$$\frac{1}{\rho} (E(\mathbf{x}_i) - E(\mathbf{x}_0)) = \int_R (\mathbf{u} \times \boldsymbol{\omega}) \cdot \nabla \psi dV + \int_S \psi \frac{\partial \mathbf{u}}{\partial t} \cdot \mathbf{n} dS$$

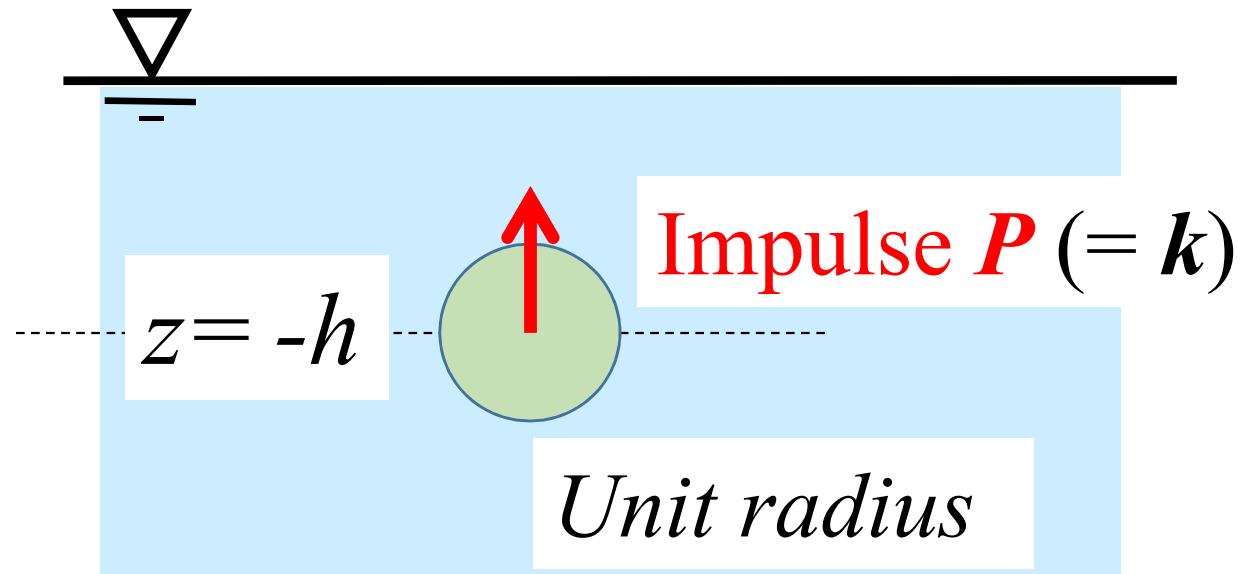
and this,

... to estimate this.



Numerical **TEST** of inversion (dynamic relation)

Consider a vertically oriented **Hill's spherical vortex**, introduced *instantaneously* under a flat, free surface (semi-infinite bath).

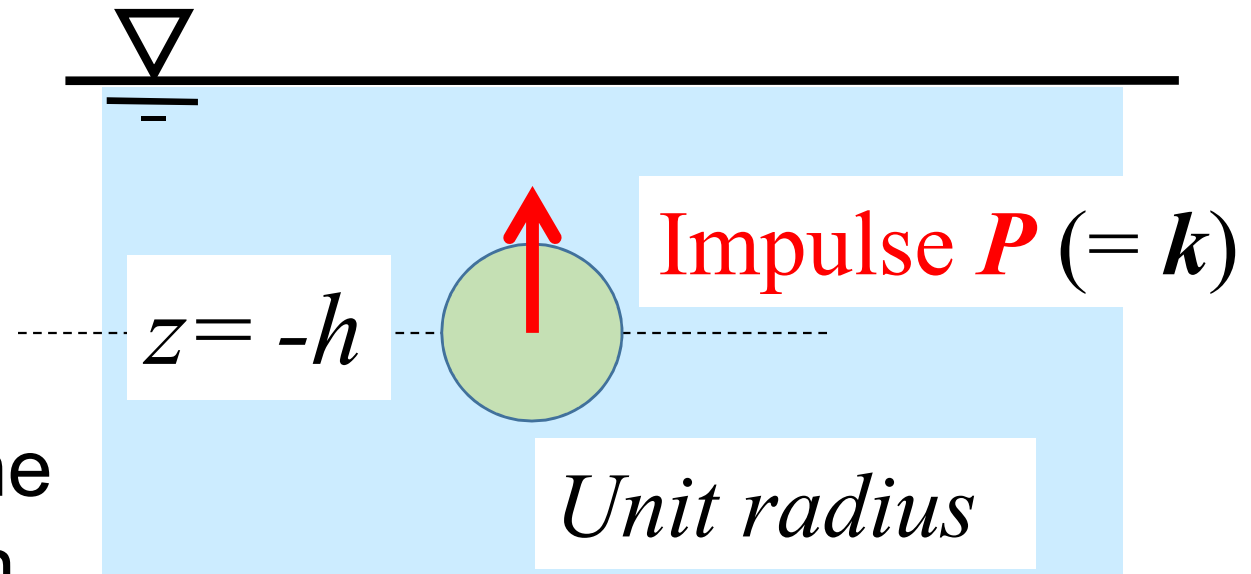


The dynamic relation requires the surface distribution of $\frac{\partial w}{\partial t}$.

TEST inversion of dynamic relation

vertically oriented Hill's spherical vortex, introduced instantaneously ...

The dynamic relation requires the surface distribution of $\frac{\partial w}{\partial t}$.

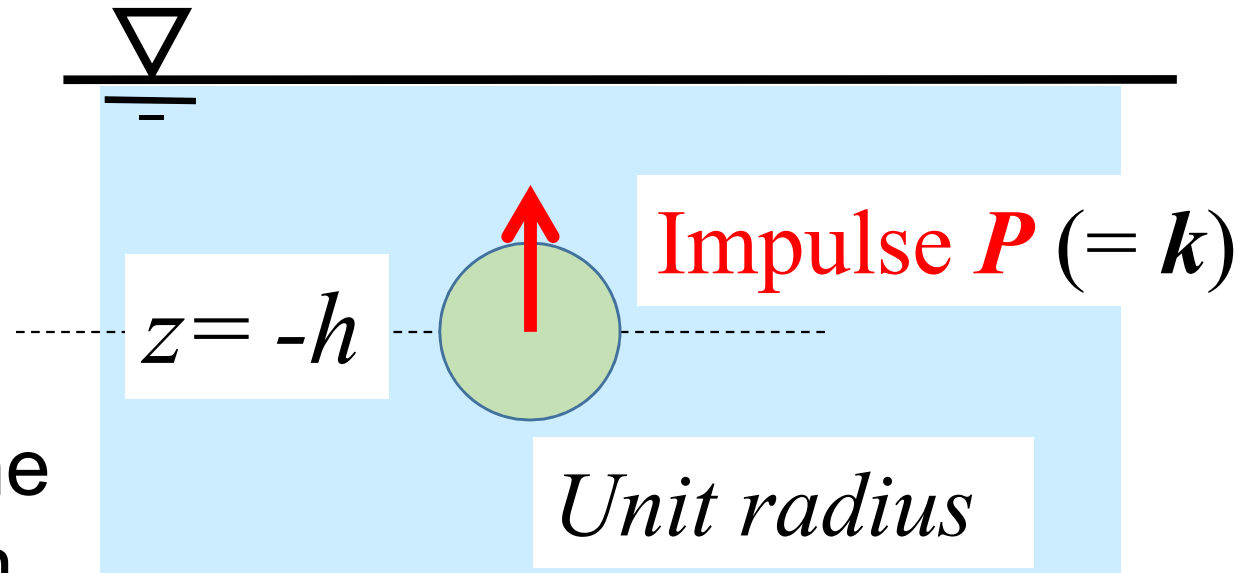


This can be obtained, in this simple geometry, by specifying the analyzing flow as due to a vertical dipole at the surface. Then
$$\frac{\partial w}{\partial t} = \int_R (\mathbf{u} \times \boldsymbol{\omega}) \cdot \nabla \tilde{\psi} dV$$

TEST inversion of dynamic relation

vertically oriented Hill's spherical vortex, introduced instantaneously ...

The dynamic relation requires the surface distribution of $\frac{\partial w}{\partial t}$.

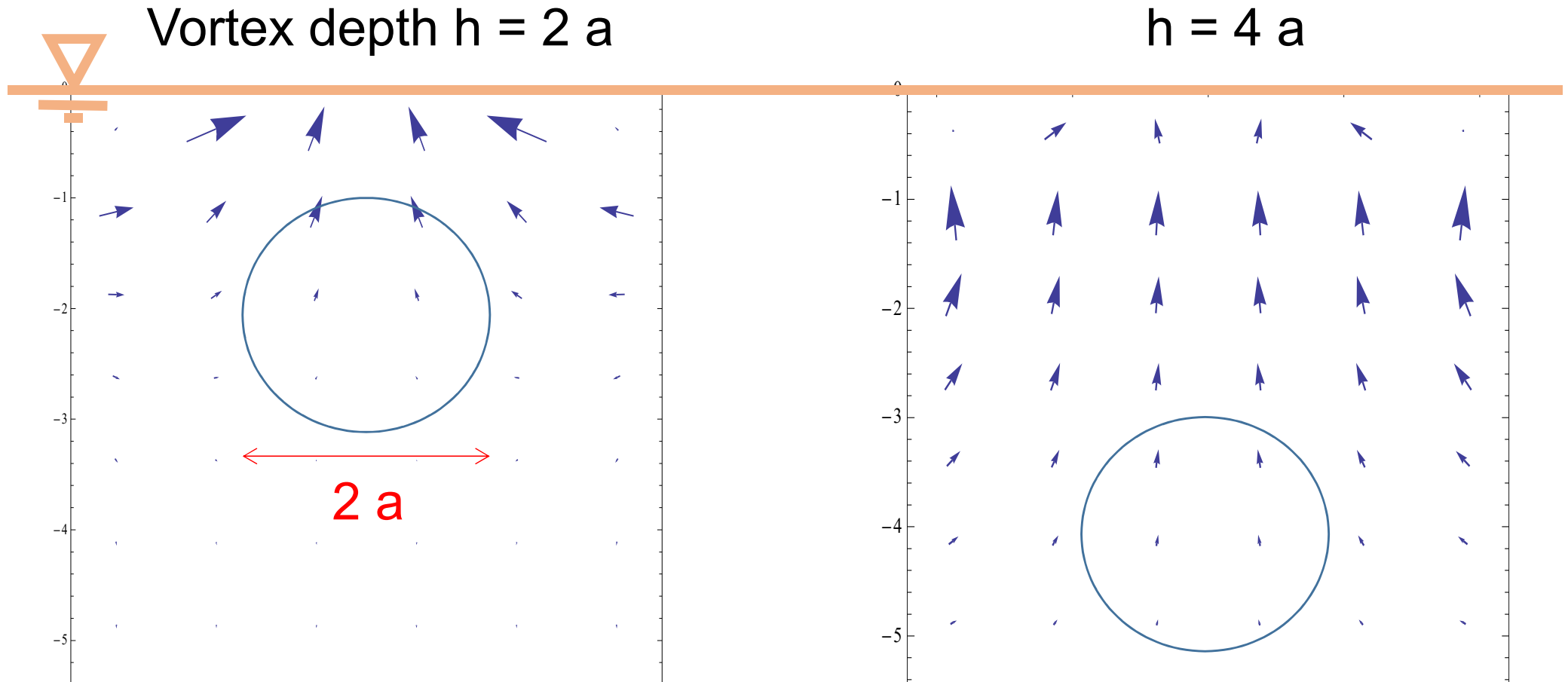


This can be obtained, in this simple geometry, by specifying the analyzing flow as due to a vertical dipole at the surface. Then

$$\frac{\partial w}{\partial t} = \int_R (\mathbf{u} \times \boldsymbol{\omega}) \cdot \nabla \tilde{\psi} dV$$

PRELIMINARY **RESULTS** of inversion of
 (not “original” eqn.) for subsurface $\mathbf{u} \times \boldsymbol{\omega}$

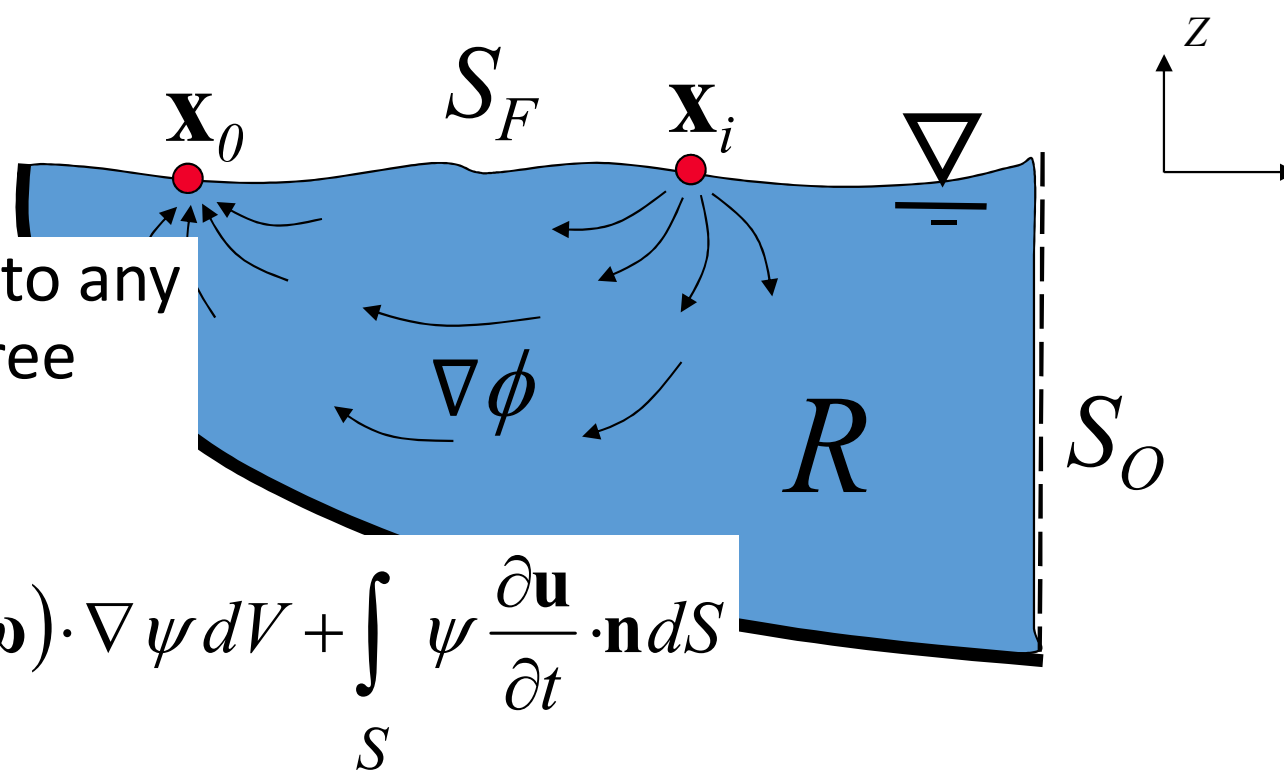
$$\frac{\partial w}{\partial t} = \int_R (\mathbf{u} \times \boldsymbol{\omega}) \cdot \nabla \tilde{\psi} dV$$



“Overdetermined” inversion, NO NOISE ADDED to “measurements”;
 $32^2 = 1024$ surface points to estimate $3 \cdot 324$ components of $\mathbf{u} \times \boldsymbol{\omega}$
 “Zero-order regularization” of normal equations (Press *et al.*, *NumRec*)

Conclusion

- The *kinematic* results apply to any incompressible flow with a free surface



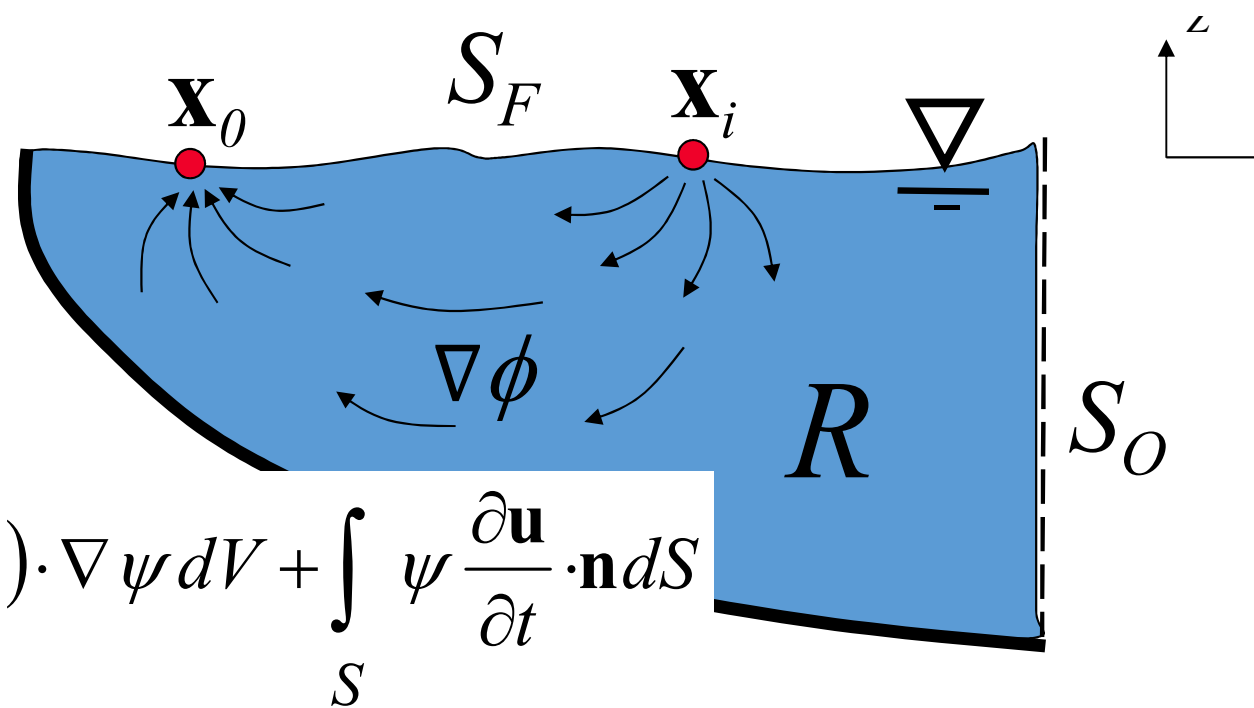
$$\frac{1}{\rho}(E(\mathbf{x}_i) - E(\mathbf{x}_0)) = \int_R (\mathbf{u} \times \boldsymbol{\omega}) \cdot \nabla \psi dV + \int_S \psi \frac{\partial \mathbf{u}}{\partial t} \cdot \mathbf{n} dS$$

The *dynamic* results apply only to flows with negligible density variations.

Generally, surface waves will propagate into the observational region. In principle, these effects are included, but how to estimate integral over S_0 ?

Conclusion (2)

- The *kinematic* results apply to any incompressible flow with a free surface



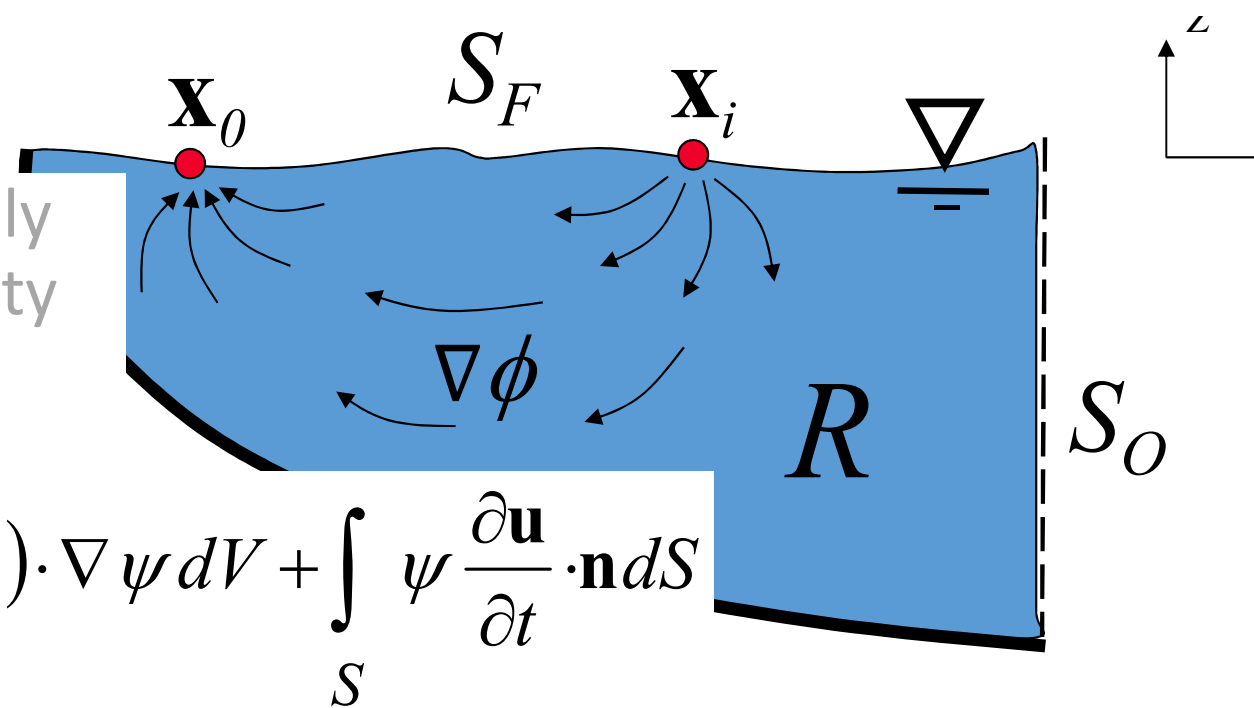
$$\frac{1}{\rho}(E(\mathbf{x}_i) - E(\mathbf{x}_0)) = \int_R (\mathbf{u} \times \boldsymbol{\omega}) \cdot \nabla \psi dV + \int_S \psi \frac{\partial \mathbf{u}}{\partial t} \cdot \mathbf{n} dS$$

The *dynamic* results apply only to flows with negligible density variations. Viscosity yields an additional surface term (useful for microfluidic PIV, etc?)

Initial tests of the **inversion** of subsurface field of $(\mathbf{u} \times \boldsymbol{\omega})$, for a Hill vortex, **smear out the true field, but did reflect differences in the vortex depth** ($h=2$ vs. $h=4$). Need to investigate nonuniqueness of dynamic relation.

Conclusion (3)

- The *dynamic* results apply only to flows with negligible density variations.



$$\frac{1}{\rho}(E(\mathbf{x}_i) - E(\mathbf{x}_0)) = \int_R (\mathbf{u} \times \boldsymbol{\omega}) \cdot \nabla \psi dV + \int_S \psi \frac{\partial \mathbf{u}}{\partial t} \cdot \mathbf{n} dS$$

In the context of “nowcasting” flow **with a Kalman filter**, such **equations would be used in “forward mode”**, *i.e.* compute LHS given RHS from currently estimated state variables. Also, could **tailor $\nabla\psi$ to our empirical basis functions**.

Future work;

Possible to extend dynamic result to stratified flow?

Thanks! ご清聴ありがとうございます。